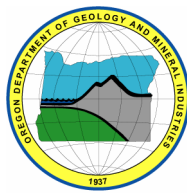

State of Oregon
Department of Geology and Mineral Industries
Vicki S. McConnell, State Geologist

**OPEN-FILE REPORT
O-06-07**

**PRELIMINARY GEOLOGIC MAP OF THE SPRINGFIELD
7.5' QUADRANGLE, LANE COUNTY, OREGON**

By

Frank R. Hladky and Glenn R. McCaslin
Oregon Department of Geology and Mineral Industries



2006

NOTICE

This paper is being published as received from the author(s). No warranty, expressed or implied, is made regarding the accuracy or utility of the information described and/or contained herein, nor shall the act of distribution constitute any such warranty. This disclaimer applies both to individual use of the data and aggregate use with other data. The Oregon Department of Geology and Mineral Industries shall not be held liable for improper or incorrect use of this information.

This publication is a U.S. Geological Survey STATEMAP 2003 deliverable.

Oregon Department of Geology and Mineral Industries Open File Report
Published in conformance with ORS 516.030

For copies of this publication or other information about Oregon's geology and natural resources, contact:

Nature of the Northwest Information Center
800 NE Oregon Street #5
Portland, Oregon 97232
(503) 872-2750
<http://www.naturenw.org>

Preliminary Geologic Map of the Springfield Quadrangle, Lane County, Oregon

Introduction

The Eugene-Springfield Urban Area is Oregon's second largest and is home to a large and rapidly growing population. The adjacent cities of Eugene and Springfield have a combined 2000 population of over 190,000, and a growth rate over the last ten years greater than 20%. Population growth and development have also been rapid in the small towns and rural areas around the two major cities. Managing growth and development requires good geologic information for engineering, to manage landslide, flood and erosion hazards and to properly develop and regulate heavily used groundwater resources. The Springfield quadrangle is one of several new, detailed 1:24,000 scale maps being completed for the Eugene-Springfield urban area by the Oregon Department of Geology and Mineral Industries. Funding for the project is from the State of Oregon and the U.S. Geological Survey through the STATEMAP portion of the National Cooperative Geologic Mapping Program under assistance award #02HQAG2037. *"The views and conclusions contained in this document are those of the authors and should not be interpreted as necessarily representing the official policies, either expressed or implied, of the U.S. Government."* Funding for McCaslin was provided through a mentorship program of the Association of American State Geologists through a grant from the National Science Foundation.

The study area (Figure 1) is located at the southern end of the Willamette Valley in western Oregon. The area is entirely within Lane County. Four rivers, the Middle Fork Willamette, Coast Fork Willamette, McKenzie, and the Mohawk, converge within the quadrangle. In addition to the heavily urbanized areas of Springfield, the area includes dense rural residential areas in the surrounding hills, intensively farmed lands in the valleys, and privately owned and public timberland in the upland areas.

The regional geology consists of three general domains. West of the quadrangle, the Coast Range foothills are predominantly composed of Eocene to Oligocene marine and continental sedimentary and volcanoclastic rocks of the Spencer, Eugene, and Fisher Formations, with minor basaltic sills (Madin and Murray, 2004). The Eugene Formation (marine nearshore sandstone) and Fisher Formation (volcanoclastic sandstone, lahars and basalt flows) interfinger. The foothills of the Cascade Range are composed of Oligocene to Miocene volcanic and volcanoclastic rock and associated tuffaceous sedimentary rocks, intrusions and vent complexes. The dominant structure is a slight to moderate dip to the east, broken by high-angle faults. Between the Coast Range and the Cascade Range, is the Willamette Valley which is filled with Quaternary sediment, including older alluvium and volcanic debris flows, multiple ages of fluvial terraces, silt deposited by catastrophic Missoula floods, and modern alluvium in the channel and meander belt of the Willamette River.

Methods

This geologic map was prepared using a variety of data including existing mapping, new field observations, high resolution topographic data, geochemistry, petrography, isotopic age data, and air photo interpretation using a PG-2 photogrammetric plotter.

Understanding of the geology of the Eugene-Springfield area is based mainly upon Vokes and others (1951) map at 1:62,500. Maddox (1965) prepared a 1:31,250 geologic map of the Springfield urban area that covers all of the quadrangle except for the Mohawk valley and the Coburg Hills. A master's thesis map of the Coburg Hills at 1:62,500 touches the northwest corner of the map (Lewis, 1951). Regional geologic maps range from 1:100,000 to 1:250,000 scale (Peck, 1960; Peck and others, 1964; Walker and Duncan, 1989; Yeats and others, 1996; O'Connor and others, 2001).

New field data was collected throughout the quadrangle. Much of the geology is obscured by urbanization in the valleys. In upland areas, many of the bedrock units are deeply weathered to saprolitic soils, particularly in the Coburg Hills, Camp Creek Ridge, and northeast of Jasper, complicates mapping of units. Contacts were rarely observed, but could be deduced by changes in topography and lithology of

colluvial hillwash between bedrock exposures. Exposure of units was facilitated where there were roadcuts in suburban developments and along logging roads. Otherwise, thick vegetation, often dominated by poison oak and blackberries, usually covered the landscape. Access in urban and suburban areas was facilitated by numerous roads and sidewalks. Much of the upland areas are owned by the Weyerhaeuser and Giustina timber companies, both of which graciously provided keys to their road networks.

Approximately 200 samples were collected and examined, 38 samples were analyzed for major oxides and trace elements (Table 1) and one new sample was analyzed for its isotopic age (Table 2). Additional samples with locations and lithologic identifications are in Appendix A. Detailed XRF methodology is in Appendix B. Detailed $^{40}\text{Ar}/^{39}\text{Ar}$ procedures and interpretation for the new isotopic age are in Appendix C. The new isotopic date adds to the many dates in the region compiled by Retallack and others (in Prep.) (Figure 2). Paleontological characteristics provide a basis for discriminating the Eugene and Fisher Formations in the region and have been the focus of studies by Vokes and others (1951), Hickman (1969), and Retallack and others (in Prep.), however, no additional paleontological studies were carried out for this map.

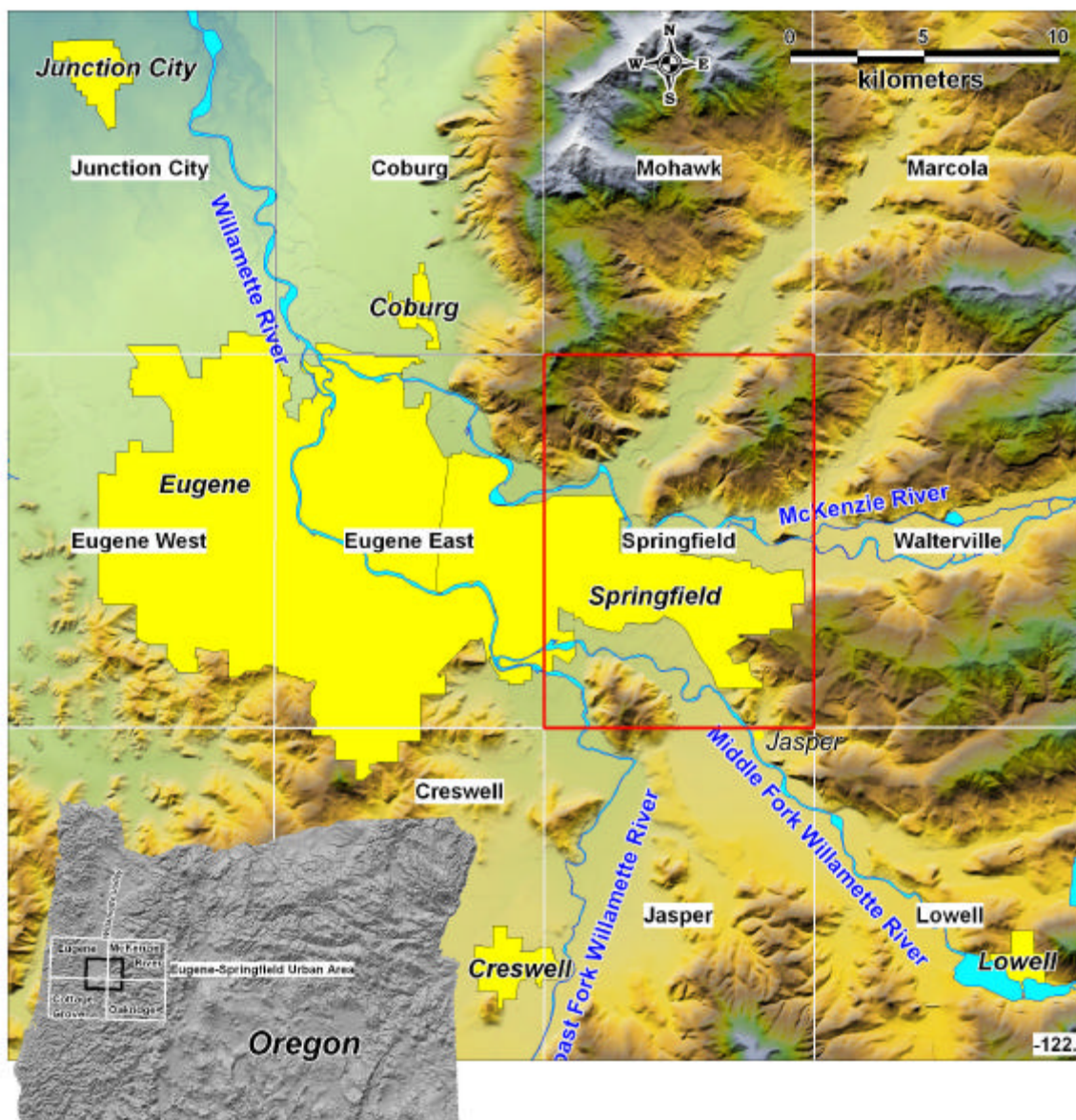


Figure 1. Eugene urban area location map. Springfield quadrangle bordered in red.

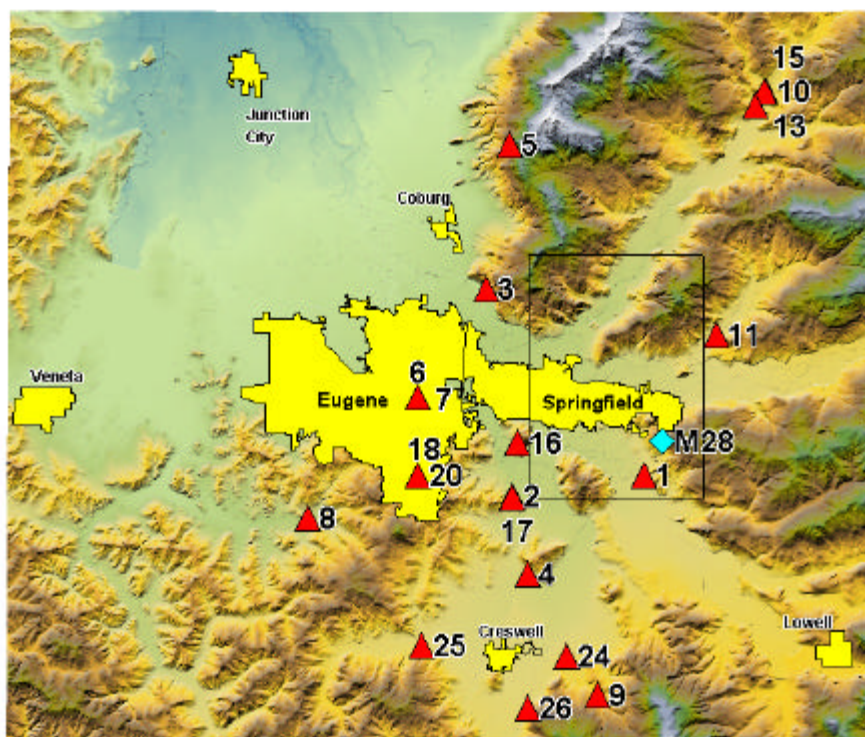


Figure 2. Location map of isotopic ages compiled in Table 2. Springfield quadrangle outlined in black.

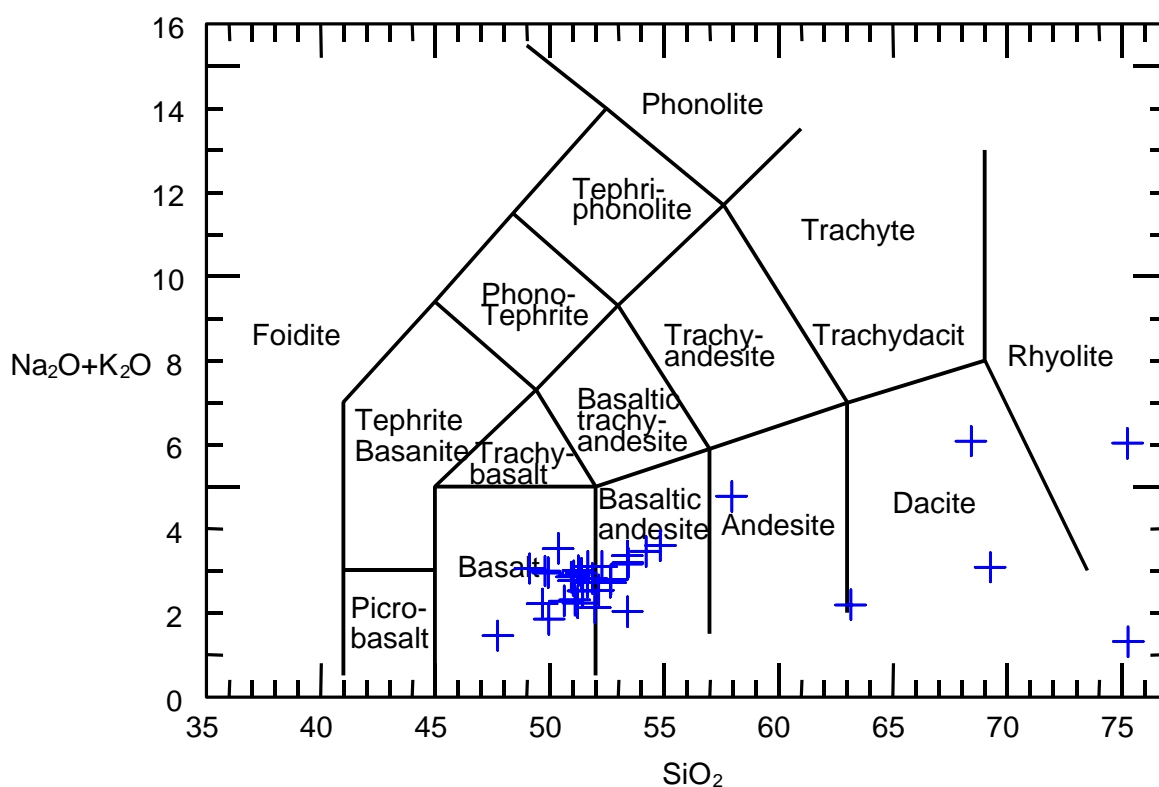


Figure 3. Le Bas and Streckeisen (1991) TAS (total alkalis vs. silica) classification for all rocks from Table 1. Volcanic rocks in the Springfield quadrangle range from basalt to rhyolite in composition.

Table 1. Whole-rock analyses, Springfield quadrangle, Lane County, Oregon. Major oxides reported in weight percent; trace elements in ppm. XRF analyses by the laboratory of Stanley A. Mertzman, Franklin and Marshall College, Lancaster, PA. Eastings and northings are referable to 1927 North American datum, Universal Transverse Mercator projection for continental United States, zone 10. All samples are from the Springfield quadrangle, except M22, which is immediately to the west.

Map No	SAMPLE	UNIT	NAME	UTM_N	UTM_E	LITHOLOGY	COMMENTS	QUADRANGLE
M13	SF44	Tb	basalt and basaltic andesite (Oligocene)	4881074	500318	basaltic andesite	Coburg Hills	Springfield
M22	SF030703-1	Tb	basalt and basaltic andesite (Oligocene)	4875566	499808	fine-grained basalt	Springfield Quarry	Eugene East
M23	SF139	Tb	basalt and basaltic andesite (Oligocene)	4876039	503285	basalt	--	Springfield
M24	SF135	Tb	basalt and basaltic andesite (Oligocene)	4875538	504128	basaltic andesite	Mt. Vernon	Springfield
M9	SF28	Tbac	basalt of Camp Creek Ridge	4883606	509180	basalt	Camp Creek Ridge	Springfield
M11	SF030721-3	Tbac	basalt of Camp Creek Ridge	4882776	509077	fine-grained basalt	Camp Creek Ridge	Springfield
M20	SF030702-2	Tbac	basalt of Camp Creek Ridge	4879474	507685	fine-grained basalt	Bellinger Landing	Springfield
M21	SF030702-1	Tbac	basalt of Camp Creek Ridge	4878711	509115	fine-grained basaltic andesite	Camp Creek butte	Springfield
M1	SF90	Tbah	basalt of Coburg Hills	4885355	501975	fine grained andesite	Coburg Hills	Springfield
M2	SF030624-1	Tbah	basalt of Coburg Hills	4884486	500019	fine-grained basalt	Top of Coburg Ridge	Springfield
M38	SF030725-2	Tbd	basaltic dike	4871895	507911	fine-grained basalt	Dike	Springfield
M15	SF030729-2	Tbm	basalt of Mohawk	4879782	502763	fine-grained basalt	Vitus Butte	Springfield
M17	SF030702-4	Tbm	basalt of Mohawk	4879470	503010	medium-grained basalt	Hayden Bridge	Springfield
M18	SF030707-2	Tbm	basalt of Mohawk	4879485	503920	fine-grained basalt	"Mohawk"	Springfield
M31	SF87	Tbmp	basalt of Mt. Pisgah	4873382	501491	basalt	Mt. Pisgah	Springfield
M32	SF76	Tbmp	basalt of Mt. Pisgah	4873473	502277	basalt agglutinate	Mt. Pisgah	Springfield
M33	SF158	Tbmp	basalt of Mt. Pisgah	4872733	501561	pyroxene basalt	Mt. Pisgah	Springfield
M34	SF85	Tbmp	basalt of Mt. Pisgah	4872815	502670	altered basaltic agglutinate	Mt. Pisgah	Springfield
M35	SF82	Tbmp	basalt of Mt. Pisgah	4872302	502971	basaltic andesite	Mt. Pisgah	Springfield
M36	SF162	Tbmp	basalt of Mt. Pisgah	4871841	503735	f.g.basalt	Mt. Pisgah summit area	Springfield
M27	SF030723-4	Tdxt	tuff of Dexter	4874970	506520	rhyolitic pumice lapilli tuff	Dexter tuff	Springfield
M37	SF030724-2	Tdxt	tuff of Dexter	4872514	506938	dacitic pumice lapilli tuff	Dexter tuff	Springfield
M25	SF030709-2	Tmba	basaltic andesite (Miocene)	4875773	506432	aphanitic basaltic andesite	"57th St quarry"	Springfield
M28	SF8	Tmba	basaltic andesite (Miocene)	4874930	507596	columnar basaltic andesite	Natron Quarry	Springfield
M29	SF146	Tomb	basaltic andesite (Oligocene and Miocene)	4874978	508892	basaltic andesite	Little Butte Wallace Creek	Springfield
M30	SF145	Tomb	basaltic andesite (Oligocene and Miocene)	4874519	508647	basaltic andesite	Little Butte Wallace Creek	Springfield
M4	SF13	Tpb	pyroxene basalt	4884796	507929	pyroxene basalt	Camp Creek Ridge	Springfield
M6	SF16	Tpb	pyroxene basalt	4884398	507502	pyroxene basalt	Camp Creek Ridge	Springfield
M8	SF030630-2	Tpb	pyroxene basalt	4883405	507280	pyroxene basalt	Alder Branch	Springfield
M12	SF030701-3	Tpb	pyroxene basalt	4881722	506220	pyroxene basalt	Camp Creek Ridge	Springfield
M14	SF030722-3	Tpb	pyroxene basalt	4880296	504571	fine-grained basalt	"Mohawk"	Springfield
M16	SF030728-2	Tpb	pyroxene basalt	4879640	503030	pyroxene basaltic andesite	Hayden Bridge	Springfield
M19	SF030729-1	Tpb	pyroxene basalt	4879077	502337	pyroxene basalt	Vitus Butte	Springfield
M3	SF68	Tr	rhyolite	4884480	503044	altered dacite	Coburg Hills	Springfield
M7	SF030701-1	Tr	rhyolite	4883230	506140	light gray rhyolite	Stafford Creek	Springfield
M10	SF030701-2	Tr	rhyolite	4882738	506060	agglutinous rhyolite lava	Sister Creek	Springfield
M5	SF19	Tvc	volcaniclastic rocks	4884884	508971	tuffaceous basaltic conglomerate	Camp Creek Ridge	Springfield
M23	SF030709-1	Twc	volcaniclastic rocks at Wallace Creek	4875990	507310	volc lithic clayey sandstone	Wallace Creek fm	Springfield

Table 1. (cont.)

Map No	UNIT	SiO2	TiO2	Al2O3	Fe2O3	FeO	MnO	MgO	CaO	Na2O	K2O	P2O5	LOI	Total	Fe2O3T*
M13	Tb	51.66	1.04	17.17	3.225252	5.97	0.16	6.03	10.34	2.14	0.52	0.15	1.17	99.57525	9.86
M22	Tb	49.79	1.25	16.38	4.268657	5.67	0.16	6.55	9.48	2.43	0.56	0.24	2.64	99.41866	10.57
M23	Tb	50.07	1.21	14.74	4.763239	5.09	0.17	7.82	11.3	1.87	0.58	0.15	2.08	99.84324	10.42
M24	Tb	51.18	1.06	14.55	3.408593	5.94	0.16	7.56	10.7	2.09	0.61	0.21	2.07	99.53859	10.01
M9	Tbac	49.79	1.47	16.37	4.354203	5.71	0.2	5.87	10.52	2.27	0.57	0.2	2.19	99.5142	10.7
M11	Tbac	50.59	1.13	14.1	4.549877	5.21	0.16	9.22	10.05	1.99	0.75	0.23	1.78	99.75988	10.34
M20	Tbac	49.24	1.38	16.23	4.723217	5.18	0.17	5.8	10.75	2.3	0.58	0.2	3.16	99.71322	10.48
M21	Tbac	51.88	1.43	16.32	3.955103	6.6	0.19	4.1	9.81	2.57	0.49	0.22	1.98	99.5451	11.29
M1	Tbah	55.66	1.91	15.35	8.417197	2.45	0.23	1.98	5.93	3.56	1.01	0.37	2.86	99.7272	11.14
M2	Tbah	48.17	1.69	15.53	3.22	7.96	0.18	7.19	9.64	2.24	0.6	0.37	3.1	99.89	12.07
M38	Tbd	49.82	1.17	14.38	1.271315	8.52	0.17	8.3	11.55	1.66	0.58	0.19	1.83	99.44132	10.74
M15	Tbm	49.68	1.21	15.69	3.699642	6.2	0.17	6.6	11.55	1.98	0.71	0.22	1.99	99.69964	10.59
M17	Tbm	48.92	1.22	15.74	6.131353	3.67	0.15	6.22	11.61	1.96	0.77	0.23	3.07	99.69135	10.21
M18	Tbm	48.08	0.77	12.02	4.104224	5.62	0.15	14.88	9.07	1.32	0.45	0.14	3.21	99.81422	10.35
M31	Tbmp	51.04	1.06	15.08	3.841912	6	0.16	7.14	11.29	1.9	0.58	0.15	1.77	100.0119	10.51
M32	Tbmp	48.53	1.19	15.97	4.83431	5.26	0.18	6.85	11.13	1.98	0.2	0.18	3.35	99.65431	10.68
M33	Tbmp	49.93	1.01	15.42	5.192274	4.47	0.19	6.84	11.33	1.83	0.2	0.14	2.81	99.36227	10.16
M34	Tbmp	47.16	0.82	14.53	8.263191	0.6	0.12	5.06	10.63	1.22	0.56	0.15	11.2	100.31	8.93
M35	Tbmp	49.79	1.27	16.11	4.637543	5.68	0.19	5.85	11.12	2.05	0.38	0.14	2.12	99.33754	10.95
M36	Tbmp	49.63	1.04	14.71	5.374395	4.9	0.18	9.37	9.89	1.74	0.42	0.14	2.16	99.55439	10.82
M27	Tdxt	66.07	0.82	12.25	2.405482	0.31	0.04	1.09	3.82	0.77	0.38	0.04	12.02	100.0155	2.75
M37	Tdxt	63.01	0.79	13.07	4.518609	1.18	0.12	1.37	4.38	2.18	0.62	0.2	8.78	100.2186	5.83
M25	Tmba	53.58	1.79	14.83	3.714783	7.95	0.27	3.85	8.35	2.91	0.6	0.23	1.41	99.48478	12.55
M28	Tmba	51	1.71	17.04	2.036861	8.56	0.18	4.15	9.83	2.5	0.52	0.23	1.67	99.42686	11.55
M29	Tomb	52.33	1.43	17.4	4.425231	6.06	0.19	3.49	9.74	2.71	0.41	0.19	1.7	100.0752	11.16
M30	Tomb	51.82	1.49	16.54	4.626238	6.5	0.18	3.67	9.23	2.79	0.46	0.19	2.12	99.61624	11.85
M4	Tpb	47.76	1.14	16.34	8.648417	1.99	0.22	6.27	9.79	2.24	1.1	0.16	3.65	99.30842	10.86
M6	Tpb	46.76	1.17	17.41	8.410559	2.33	0.17	5.48	11.2	2.11	0.79	0.17	3.53	99.53056	11
M8	Tpb	48.68	1.25	16.22	4.34	5.73	0.16	6.91	11.74	2.09	0.83	0.26	1.35	99.56	10.71
M12	Tpb	50.71	1.01	15.04	4.542168	4.92	0.16	8.01	11.42	1.94	0.73	0.18	1.35	100.0122	10.01
M14	Tpb	48	0.91	12.56	4.988806	5.04	0.15	13.58	9.58	1.44	0.69	0.16	2.54	99.63881	10.59
M16	Tpb	52.35	1.78	14.53	6.607501	5.86	0.23	3.85	8.44	2.81	0.53	0.23	2.9	100.1175	13.12
M19	Tpb	49.43	1.23	15.19	5.305508	4.89	0.16	6.8	11.33	1.92	0.87	0.21	2.27	99.60551	10.74
M3	Tr	65.58	0.7	14.48	2.847219	2.36	0.24	0.63	3.3	4.55	1.27	0.18	3.52	99.65722	5.47
M7	Tr	76.88	0.34	11.98	1.160815	1.25	0.04	0.1	0.67	1.42	1.49	0.02	4.09	99.44082	2.55
M10	Tr	73.82	0.34	12.8	2.242142	0.34	0.06	0.63	2.11	3.73	2.18	0.06	1.67	99.98214	2.62
M5	Tvc	40.28	0.95	13.83	7.426148	2.19	0.15	8.39	10.55	0.98	0.24	0.14	15.08	100.2061	9.86
M23	Twc	54.86	1.5	15.93	6.909915	0.36	0.14	1.67	4.07	1.58	0.32	0.21	12.85	100.3999	7.31

* Fe2O3T determined by titration after the method of Reichen and Fahey (1962).

Table 1. (cont.)

Map No	UNIT	Rb	Sr	Y	Zr	V	Ni	Cr	Nb	Ga	Cu	Zn	Co	Ba	La	Ce	U	Th	Sc	Pb
M13	Tb	12	404	16.7	79	268	37	84	5.9	18.8	160	80	32	148	6	16	0.5	0.6	35	8
M22	Tb	10.5	524	20.6	99	236	78	135	8.8	21.1	227	82	40	199	11	24	<0.5	<0.5	26	6
M23	Tb	10.1	447	17.3	67	302	67	286	5.3	18	141	70	38	136	6	13	<0.5	0.8	35	6
M24	Tb	16.1	761	15.9	92	284	69	337	6.6	18.3	121	84	39	293	20	45	<0.5	3.8	33	6
M9	Tbac	8.6	643	24.4	99	306	33	67	7	20.5	235	79	34	338	20	45	2.6	4.1	33	7
M11	Tbac	13.4	592	16.6	85	273	104	371	6.7	16.9	187	81	43	212	14	31	0.9	1.3	31	5
M20	Tbac	6	572	21.5	92	311	32	58	7.1	19.9	282	79	33	197	17	36	0.5	3.1	34	6
M21	Tbac	13.2	348	22.7	88	306	15	37	9.5	19.8	107	95	29	197	14	31	<0.5	0.9	36	5
M1	Tbah	24	316	49.5	204	144	5	4	17.8	22.5	59	146	20	344	31	59	<0.5	1.4	31	8
M2	Tbah	12.2	371	25.9	162	240	83	235	12	19.2	162	95	41	229	15	34	<0.5	1.1	29	4
M38	Tbd	7.4	606	18.1	68	287	86	350	4.5	17.2	149	73	42	297	12	25	1.1	2.4	33	5
M15	Tbm	9.2	613	19.5	81	313	39	144	5.9	18.9	279	76	34	353	14	33	1.3	1	35	6
M17	Tbm	9.5	632	19.3	80	311	39	132	6.6	18.1	203	71	34	356	12	30	<0.5	2.2	34	8
M18	Tbm	6.8	471	14	56	225	518	1365	3.9	12.8	233	71	57	217	11	22	<0.5	2.5	31	5
M31	Tbmp	10.2	446	16.3	65	305	42	181	4.9	17.6	135	73	37	128	9	18	<0.5	1.1	34	6
M32	Tbmp	4.1	403	20.8	78	279	48	146	5.8	18.2	104	74	37	115	9	22	<0.5	1	36	5
M33	Tbmp	3.4	470	17.3	61	328	32	154	4.6	18.3	154	81	31	139	13	26	0.9	0.9	36	5
M34	Tbmp	7	528	12.8	49	174	24	131	3.7	14.1	82	61	27	130	6	13	<0.5	0.7	31	4
M35	Tbmp	6.8	417	20.3	78	321	28	82	5.6	20.5	184	77	34	125	9	20	<0.5	1.4	37	6
M36	Tbmp	9.6	326	15.1	60	285	108	465	4.6	16.7	118	83	44	128	4	9	<0.5	1	36	5
M27	Tdxt	8	937	15.4	119	70	3	7	6.7	10.6	95	42	4	881	1	3	0.6	0.9	21	3
M37	Tdxt	17.7	343	32.8	169	73	5	19	15.5	17.8	20	103	9	545	20	49	0.7	1.9	24	7
M25	Tmba	16.6	352	25.5	103	350	13	36	9.1	19.3	99	104	27	217	9	22	<0.5	0.7	38	7
M28	Tmba	17.2	370	23.5	91	301	16	80	8.4	20	66	98	28	208	10	23	<0.5	1.7	35	6
M29	Tomb	12.4	371	23.1	79	301	8	25	8.7	20	92	97	31	244	13	27	<0.5	1.1	39	6
M30	Tomb	11.4	345	22.5	83	304	9	24	8.7	19.9	97	95	29	179	11	23	<0.5	2.1	37	5
M4	Tpb	20.1	537	17.7	68	244	49	94	5.1	17.8	104	84	39	290	12	27	<0.5	1.9	27	4
M6	Tpb	10.5	646	17.8	71	291	45	91	4.6	19.3	115	78	40	268	13	31	<0.5	<0.5	31	5
M8	Tpb	12.6	831	18.1	78	312	45	142	6.4	18.8	213	76	37	384	20	47	<0.5	4	33	6
M12	Tpb	13.2	617	14.8	67	296	57	267	4.8	17.6	96	76	39	232	14	30	1	3.9	35	7
M14	Tpb	12.2	534	18.7	70	235	392	1210	5	14	210	76	55	551	22	48	1.9	7.6	33	9
M16	Tpb	11.1	337	26.3	102	368	10	29	9	20	214	106	30	209	13	29	<0.5	<0.5	39	7
M19	Tpb	13.2	596	27.5	79	288	50	176	6	18	205	69	37	363	16	35	0.9	0.9	34	4
M3	Tr	25.4	256	36	237	30	4	4	16.8	18.3	10	88	5	361	23	49	0.7	2.4	17	8
M7	Tr	35.3	61	14.7	201	19	6	9	11.6	14.1	10	25	3	332	9	16	1.2	3.2	6	6
M10	Tr	50	155	26.1	190	33	11	8	13.1	14	76	32	4	499	20	47	1.2	3.4	8	8
M5	Tvc	5.3	855	13.9	53	240	121	362	3.2	10.7	115	71	41	125	16	32	<0.5	1	34	5
M23	Twc	8.6	782	18.9	146	173	6	24	8.8	20	135	103	10	1728	13	28	1	1.8	40	5

Table 2. Isotopic ages in the Eugene-Springfield area after Retallack and others (in Prep.) and a new age from this study (Map No. M28, Table 1). Map numbers are keyed to Figure 2. Samples 1-8 and M28 are $^{40}\text{Ar}/^{39}\text{Ar}$ ages, the remainder are K/Ar.

Map_No.	Name	Location_Description	Legal_Description	Age_Ma
1	tuff of Dexter (unit Tdxt)	tuff of Dexter 1 mi. W Jasper railway siding	SW $\frac{1}{4}$ SE $\frac{1}{4}$ SW $\frac{1}{4}$ S10 T18S R2W Lane Co.	25.9 \pm 0.6
2	tuff of Spores Point?	tuff above Willamette flora, 0.5 mi. NE Goshen	SE $\frac{1}{4}$ NW $\frac{1}{4}$ SE $\frac{1}{4}$ S13 T18S R3W Lane Co.	30.6 \pm 0.5
3	tuff of Spores Point	tuff of Spores Point on McKenzie R. at Spores Point	NE $\frac{1}{4}$ SW $\frac{1}{4}$ NE $\frac{1}{4}$ S10 R17S R3W Lane Co.	31.3 \pm 0.6
4	Mosser Mountain tuff of Retallack and others (in Prep.)	Mosser Mountain tuff in Short Mountain landfill	NE $\frac{1}{4}$ NW $\frac{1}{4}$ NW $\frac{1}{4}$ S36 T18S R3W Lane Co.	31.8 \pm 0.8
5	tuff of Daniels Creek *	Mosser Mountain tuff 1 mi. SW Buck Mountain, Coburg Hills	SW $\frac{1}{4}$ NW $\frac{1}{4}$ NE $\frac{1}{4}$ S14 T16S R3W Lane Co.	32.3 \pm 0.6
6	tuff of Bond Creek	tuff of Bond Creek on Willamette R. N of Patterson St	SW $\frac{1}{4}$ NW $\frac{1}{4}$ NE $\frac{1}{4}$ S32 T17S R3W Lane Co.	33.9 \pm 0.7
7	tuff of Bond Creek	tuff of Bond Creek on Willamette R. N of Patterson St	SW $\frac{1}{4}$ NW $\frac{1}{4}$ NE $\frac{1}{4}$ S32 T17S R3W Lane Co.	34.8 \pm 0.2
8	tuff of Fox Hollow	Lorane Highway 0.5 m. W Spencer Grange	SE $\frac{1}{4}$ SE $\frac{1}{4}$ NW $\frac{1}{4}$ S22 T18S R4W Lane Co.	41.0 \pm 0.6
9	tuff	tuff slopes of Winberry Mountain (Millhollen, 1991)	SE $\frac{1}{4}$ NW $\frac{1}{4}$ SE $\frac{1}{4}$ S20 T29S R2W Lane Co.	21.6 \pm 1.0
10	basalt	basalt 0.5 miles south of Mabel (Lux, 1981 #41)	SE $\frac{1}{4}$ SW $\frac{1}{4}$ NE $\frac{1}{4}$ S5 T16S R1W Lane Co.	27.0 \pm 1.0
11	basalt	basalt 5 miles NE Springfield (Fiebelkorn and others, 1982 #73)	NE $\frac{1}{4}$ NE $\frac{1}{4}$ NE $\frac{1}{4}$ S24 T17S R2W Lane Co.	28.9 \pm 0.3
13	basalt	basalt 0.5 miles south of Mabel (Lux, 1981 #41)	SE $\frac{1}{4}$ SW $\frac{1}{4}$ NE $\frac{1}{4}$ S5 T16S R1W Lane Co.	28.3 \pm 1.1
15	basalt	basalt 1 mile south of Mabel (Lux, 1981 #40)	SW $\frac{1}{4}$ SE $\frac{1}{4}$ SW $\frac{1}{4}$ S5 T16S R1W Lane Co.	29.7 \pm 0.8
16	basalt	basalt of Springfield Butte quarry (Lux, 1981 #42)	NE $\frac{1}{4}$ SE $\frac{1}{4}$ SE $\frac{1}{4}$ S2 T18S R3W Lane Co.	30.3 \pm 1.1
17	tuff	tuff of Willamette Flora, Goshen Flora (Evernden & James 1964)	SE $\frac{1}{4}$ NW $\frac{1}{4}$ SE $\frac{1}{4}$ S14 T18S R3W Lane Co.	31.8 \pm 1.0
18	basalt	basalt on 40th and McDonald St, S Eugene (Lux 1981 #43)	SW $\frac{1}{4}$ SE $\frac{1}{4}$ SW $\frac{1}{4}$ S8 T18S R3W Lane Co.	32.4 \pm 0.8
20	basalt	basalt on 40th and McDonald St, S Eugene (Lux 1981 #43)	SW $\frac{1}{4}$ SE $\frac{1}{4}$ SW $\frac{1}{4}$ S8 T18S R3W Lane Co.	35.3 \pm 0.9
24	basalt	basalt 2 miles east of Creswell (Lux 1981 #24)	SW $\frac{1}{4}$ SW $\frac{1}{4}$ NE $\frac{1}{4}$ S18 T19S R2W Lane Co.	38.7 \pm 0.5
25	basalt	basalt 3 miles W Creswell (Fiebelkorn and others, 1982 #61)	NE $\frac{1}{4}$ NE $\frac{1}{4}$ NW $\frac{1}{4}$ S17 T19S R2W Lane Co.	38.7 \pm 0.5
26	basalt	basalt 2 miles SE Creswell (Lux 1981 #23)	SW $\frac{1}{4}$ NE $\frac{1}{4}$ NW $\frac{1}{4}$ S25 T19S R3W Lane Co.	39.7 \pm 1.4
M28	basaltic andesite (unit Tmba)	columnar basaltic andesite 0.7 miles NE of Natron, near Springfield	SE $\frac{1}{4}$ NE $\frac{1}{4}$ SW $\frac{1}{4}$ S3 T18S R2W Lane Co.	18.0 \pm 1.5

*The tuff at this location is a quartz-rich tuff, called the Mosser Mountain tuff by Retallack and others (in Prep.) is markedly different from the feldspar-rich tuff of Mosser Mountain originally mapped in southern Oregon (Hladky, 1992; Murray, 1994). Madin and Hladky (in Prep.) suggest the name tuff of Daniels Creek.

EXPLANATION OF MAP UNITS

Surficial Deposits

- Qal Meander-belt alluvium (Holocene)**—A complex assemblage of channelized and anastomosing mud, silt, sand, and gravel deposits mobilized during historical flooding of the Mohawk, McKenzie, and the Middle and Coast Forks of the Willamette River. The Mohawk, McKenzie, and Willamette Rivers are currently incising their beds throughout the map area. The McKenzie River, however, is currently aggrading its bed with gravel in sec. 25, T. 17 S., R. 2 W. on the east side of the map area. The meander belt is incised into braided-fan alluvium that debouches onto the plain of the Willamette Valley (Madin and Murray, 2004). O' Connor and others (2001) report ^{14}C ages of modern to 3.7 ka in the adjacent Eugene East and Eugene West quadrangles—the 3.7 ka age comes from a depth of 4 m. The gravel-rich portions of these deposits have been mined (mined areas appear on the topographic base map) to depths of 6-12 m (20-40 ft) although these quarries probably penetrate underlying braided-fan alluvium. Along the Middle Fork of the Willamette River between Springfield and Mt. Pisgah gravel has been intermittently mined, although there were no active operations during the period of this study. Similarly, gravel was mined from deposits along the McKenzie River in the vicinity of Kizer Slough. Gravel thickness is irregular and bedrock shoals to the surface cropping out in the bed of the McKenzie River near Vitus Butte, Bellinger Landing, and an unnamed butte in secs. 25 and 26, T. 17 S., R. 2 W. Bedrock also crops out in the bed of the Middle Fork of the Willamette River in sec. 7, T. 17 S., R. 2 W. on the north side of Mt. Pisgah and at several places along the northwest bank in sec. 15, T. 17 S., R. 2 W. near Jasper. The relatively sharp edge of the meander belt morphology, in most places, is the primary criteria for mapping.
- Qa Alluvium (Holocene)**—Sand and subangular to angular cobble-pebble gravel thick enough to map deposited along streams tributary to the Middle Fork of the Willamette River north of Jasper. Includes deposits along Wallace Creek in sec. 14, T. 18. S., R. 2 W. which are dominantly angular cobble-pebble gravel of basaltic andesite and deposits in an unnamed intermittent stream in sec. 9, T. 18. S., R. 2 W. that are dominantly sand and pebble gravel derived from volcanoclastic deposits. Thickness is generally less than 3 m (10 ft)
- Qc Colluvium (Pleistocene and Holocene)**—Soil-dominated, unconsolidated deposits of heterogeneous rock fragments and soil deposited by rainwash, sheetwash, or slow continuous downhill creep; obscures underlying rocks on the lower slopes of ridges. Generally, voids between rock fragments are filled with soil, rock fragments, and vegetative matter. Mappable colluvium deposits are generally located near the lower slopes of ridges. They are not fan-shaped, instead they mantle irregularly shaped hillslopes. Intermittent to perennial streams may be established on them. Mappable deposits are located in the Mohawk valley from Sister Creek to Alder Branch, on the southern slopes of Camp Creek Ridge from Bellinger Landing to Camp Creek, in east Springfield in secs. 35 and 36, T. 17. S., R. 2 W., in the Wallace Creek area of sec. 14, T. 18. S., R. 2 W., and the north slope of Mt. Pisgah in sec. 7, T. 18. S., R. 2 W. Based upon examinations of topography and roadcuts, thickness locally exceeds 10 m (30 ft).

- Qls Landslide deposits (Pleistocene and Holocene)**—Slightly consolidated chaotic mixtures of angular rock and saprolitic soil, resulting from debris flow and slump failures originating in steeper upland areas. Landslide deposits of substantial size are located in the Coburg Hills in sec. 18, T. 17. S., R. 2 W., on Camp Creek Ridge in T. 17 S., R. 2 W., and the 67th Street area of east Springfield in secs. 35 and 36, T. 17. S., R. 2 W. Steep terrain, deterioration of mafic lavas to saprolitic soils and regolith, or, as in the case at 67th Street, underlying decomposed tuff beds, correlate with the occurrence of slides. An interview with a home owner in the area of the 67th Street slide indicated that while some homes, in no particular pattern, had experienced differential settling, many, such as his 5-year old home, had not. The stability of landslide deposits is largely outside the scope of this study and best determined on a site by site basis.
- Qf Braided-fan alluvium (Pleistocene and Holocene)**—A broad, braided, channelized fan of sand and gravel deposited by the Willamette and McKenzie Rivers, the head of which extends into the Springfield quadrangle. Braided fan sediments range from silt to boulder gravel, but are mostly sandy pebble-cobble gravel. The fan form is based on high resolution DEM from 2-ft contour data (Madin and Murray, 2004). Modern overbank silts have not been discriminated in this map. Exposures in gravel pits in the adjoining Eugene East and Eugene West quadrangles reveal embedded lahars and tuffs (O'Connor and others, 2001; Madin and Murray, 2004). ⁴⁰Ar/³⁹Ar analyses on obsidian in a lahar 30 m (90 ft) from the surface yielded ages of 418 ± 10 ka and 426 ± 4 ka (O'Connor and others, 2001; Madin and Murray, 2004), although the ages may be from older gravels (Madin and Murray, 2004). Where gravel is several hundred feet thick, it may not all be unit Qf. For example, near the McKenzie River in sec. 25, T. 17 S., R. 3 W., the Springfield Utility Board Test Well #5 (4878355N, 500150E) has gravel thickness in excess of 350 ft (OWRD GRID database, Well # LANE 11370). Where gravel is hundreds of feet thick it is typically confined to channels less than a mile wide beneath the modern valley floors (Thomas J. Wiley, Oregon Dept. of Geology and Mineral Industries, 2004, personal comm.). During the most recent glaciation, the area's rivers adopted a broad, braided channel morphology but during the current interglacial period, they switched to a pattern of meander and incision (Madin and Murry, 2004).
- Qoam Older alluvium of the Mohawk River valley (Pleistocene and Holocene)**—Generally unconsolidated sand, silt, and pebble and cobble gravel deposited in the Mohawk River valley. Locally, in sec. 3, T. 17 S., R. 2 W., these gravels are partially cemented. Pebbles and cobbles are well-rounded and derived mostly from mafic lava flows. These deposits are being incised by the modern Mohawk River as much as 6 m (20 ft). In most of the valley the deposits are overlain by soil of variable thickness that either is or has been under cultivation. Includes undifferentiated, cultivated and vegetated modern silt and mud overbank deposits. Overlain by and probably interbedded with alluvial fan deposits. Coeval with aggradation of braided fan deposits of the Willamette and McKenzie Rivers. Locally, there is at least 150 ft of alluvium underlying the Mohawk River valley (Wiley, 2004, personal comm.).
- Qaf Alluvial fan deposits (Pleistocene and Holocene)**—Unconsolidated angular to subrounded cobble-boulder gravel, mud, clay and soil deposited by debris-flows originating in steep upland draws. The deposits in this unit are the result of sheet-wash, braided fluvial processes, and catastrophic downslope movements during high runoff events. Notable deposits in the Coburg Hills that debouch into the Mohawk River valley, and along Wallace Creek near Jasper. Some small alluvial fan deposits also occur on Mt. Pisgah. Local, shallow incisement of intermittent streams indicates that deposition may have been more prevalent during Pleistocene time than today.

QTtg **Terrace gravel (Pliocene?-Pleistocene)**—Tan-weathering, poorly sorted, saprolitic sand and gravel. Rounded pebbles and cobbles retain their internal texture but are penetratively weathered to soft clay; the porphyritic lithologies are the softest. Exposures are located on Mt. Vernon 26 m (85 ft) above the McKenzie River floodplain in the south-central part of the map. The gravels are incised on the north side of Mt. Vernon by the McKenzie River system. The gravels mantle topography to an unknown depth on the south slope of Mt. Vernon which slopes toward the Middle Fork of the Willamette River. The gravel at Mt. Vernon are variable in thickness and unconformably overlie volcanoclastic rocks of the Fisher Formation. Another small exposure is located in sec. 24, T. 17 S., R. 2 W. near Camp Creek and the McKenzie River. The elevation of these exposures above modern flood plains, incision by modern systems, and penetrative, saprolitic alteration indicate that the deposits are significantly older than the modern gravels.

Tertiary (Oligocene and Miocene) Volcanic Rocks

Tmba **Basaltic andesite (lower Miocene)**—Dark-gray, very fine grained basaltic andesite. Although usually massive to tabular, well-formed columns are developed at a quarry near Natron in sec. 3, T. 18 S., R. 2 W. It is exposed only in the southeast corner of the map area. Petrographically, the basaltic andesite is comprised of seriate plagioclase up to 1 mm usually smaller than 0.5 mm set in dark-gray glass which comprises 65-75 percent of

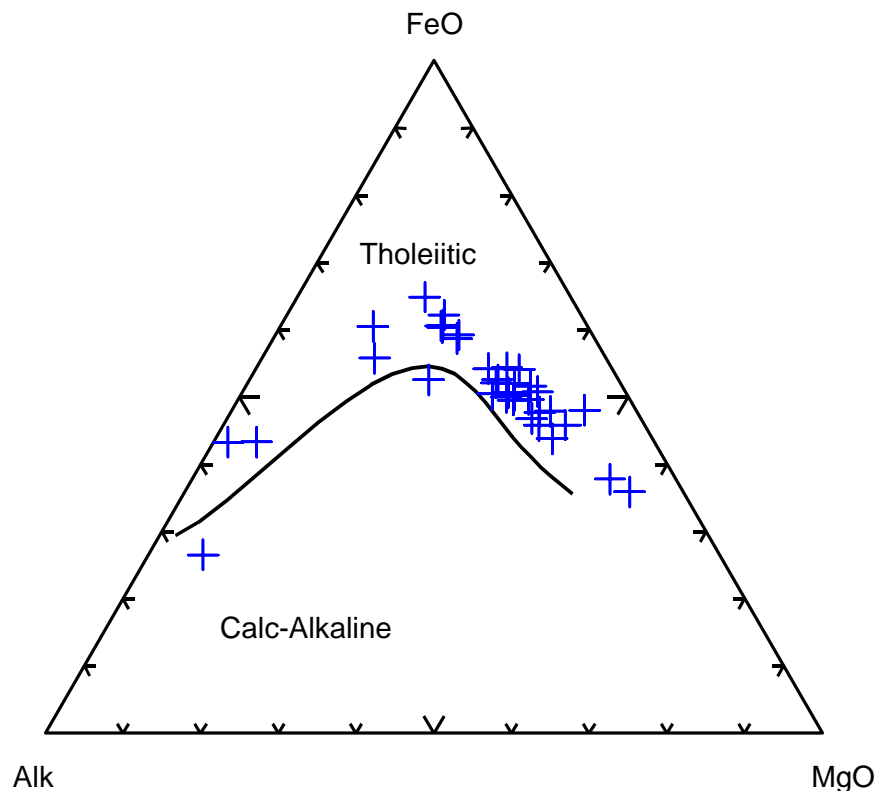


Figure 4. Irvine and Barager (1971) AFM diagram with plot of all rocks from Table 1. Volcanic rocks in the Springfield quadrangle show a clear tholeiitic trend. Silicic rocks fall on the left side. Two altered silicic samples fall within the calc-alkaline field—a sample of the tuff of Dexter and a sample of rhyolite, but otherwise these units are also tholeiitic.

the rock. Fine-grained olivine, smaller than 0.5 mm comprises 1-2 percent. Soil development varies in thickness, often only a decimeter or so in thickness, and is usually dark brown. Geochemically, the flows are basaltic andesite (Table 1, Map No.s M25, M28; Figure 3) and tholeiitic (Table 1, Figure 4). This is the youngest volcanic unit in the quadrangle and it rests disconformably on many older sedimentary and volcanoclastic units including the Fisher Formation, the tuff of Dexter, and the volcanoclastic rocks at Wallace Creek. Abrupt high angle contacts, overall map distribution, and a young age indicate this to be a canyon-filling lava. It has a new $^{40}\text{Ar}/^{39}\text{Ar}$ age of 18.0 ± 1.5 Ma (Table 2).

Tomb Basaltic andesite (upper Oligocene and lower Miocene)—Brown-weathering, dark-gray to medium-dark-brownish-gray, usually penetratively weathered, massive to tabular basaltic andesite. Commonly covered by thick red or brown saprolitic soils which mask exposures of lava flows and may mask small discontinuous interbeds of volcanoclastic rocks which, because of poor exposure, could not be reliably mapped as shown by Maddox (1965). Petrographically these flows are comprised of 70-80 percent seriate plagioclase up to 2 mm but mostly smaller than 0.5 mm, 10-20 percent dark gray glass, and 5 percent iddingsitized olivine and pyroxene usually smaller than 0.5 mm and typically weathered to orange iron oxides. Geochemically, the flows are basaltic andesite (Table 1, Map No.s M29, M30; Figure 3) and are tholeiitic (Table 1, Figure 4). Exposed in the southeast corner of the quadrangle, these flows overlie the volcanoclastic rocks at Wallace Creek.

Two Volcanoclastic rocks at Wallace Creek (upper Oligocene)—Brown, poorly sorted, volcanic lithic clayey sandstone, yellow unwelded lithic lapilli-ash tuff, petrified wood,



Figure 5. An example of volcanoclastic rocks at Wallace Creek—unit Two—brown tuffaceous polymictic pebbly mudstone with subrounded and subangular clasts.

and brown tuffaceous polymictic pebbly mudstone with subrounded and subangular clasts (Figure 5). Clasts, dominantly basalt, are ubiquitously embedded and supported by a tuffaceous muddy matrix. Pumice lapilli, where present, are rounded. These volcanoclastic sediments are derived mostly from mafic volcanic rock—the geochemistry of a clay-rich sandstone (Table 1, Map No. 23) supports this field observation. Multiple lithologies in alternating beds with abrupt contacts are often exposed in a single outcrop. Individual beds are laterally discontinuous. More resistant lithologies uphold small knolls, less resistant lithologies weather to subdued topography. The unit's composition and complexity indicate a combination of lahar, volcanoclastic debris flow, minor fluvial overbank, and hillside outwash deposits. Exposed in the southeast corner of the quadrangle, these rocks are underlain by massive to thick-bedded fluvial sandstones and conglomerates of the Fisher Formation above the tuff of Dexter. The volcanoclastic rocks at Wallace Creek are overlain by upper Oligocene-lower Miocene basaltic andesite (unit Tomb) and middle Miocene canyon-filling basaltic andesite (unit Tmba). In other parts of the region, these lithologies are collectively mapped within the Fisher Formation (Madin and Murray, 2004). Because of good exposure and consistent stratigraphic relationships to underlying fluvial sandstones in this area, however, it is possible to map these predominantly non-fluvial terrestrial volcanoclastic sediments and tuffs as a distinct unit. Thickness in the quadrangle at least 152 m (500 ft).

Tdxt Tuff of Dexter (upper Oligocene)—Medium-gray- to tan-weathering, very-light-gray to pale-yellowish-tan, dacitic to rhyolitic, pumice-rich, lithic vitric lapilli ash tuff. Pumice lapilli can be several centimeters in size; pumice lapilli commonly comprise more than half the rock. Forms massive resistant beds where unaltered and subdued topography where weathered to clays. Exposed in the southeastern corner of the quadrangle from Wallace Creek to the Springfield city limits. The tuff of Dexter is both underlain and



Figure 6. Conglomerate of the Fisher Formation locally fills channels in the scoured top of the tuff of Dexter northwest of Jasper.

overlain by well-sorted conglomeratic sandstones of the Fisher Formation along the east bank of the Middle Fork of the Willamette River (Figure 6). Locally, tuffaceous subangular conglomerate and mudstone—volcaniclastic rocks at Wallace Creek—fill channels overlying the tuff of Dexter. Geochemically, the tuff ranges from dacite to rhyolite (Table 1, Map No.s M27, M37; Figure 3), and generally follows the tholeiite trend (Figure 4). Called the Dexter tuff by Retallack and others (in Prep.), it has an $^{40}\text{Ar}/^{39}\text{Ar}$ age of 25.9 ± 0.6 Ma (Table 2). Thickness in the map area is less than 100 m (300 ft)

Tbac Basalt of Camp Creek Ridge (upper Oligocene)—Brown- to gray-weathering, dark-greenish-gray, massive to tabular fine-grained basalt. Weathering of the unit produces thick colluvium with abundant subangular basalt fragments to boulder size in dark reddish-brown or brown soil. Petrographically the basalt consists of a groundmass of seriate plagioclase to 1.5 mm, up to 50 percent glass, and olivine and clinopyroxene phenocrysts from 1-4 mm. Olivine and pyroxene are commonly partially altered to iddingsite, chlorite or green smectite clay. Geochemically, the flows are basalt (Table 1, Map No.s M9, M11, M20, M21; Figure 3) and tholeiitic (Table 1, Figure 4). The unit is broadly chemically similar to Oligocene basalt flows (unit Tb) to the west but is probably stratigraphically higher in the section. Dipping eastward as a thin-veneer, it caps Camp Creek Ridge and overlies pyroxene basalt. It also upholds a small butte at the mouth of Camp Creek in secs. 25 and 26, T. 17 S., R. 2 W. and is exposed at Bellinger Landing on the McKenzie River.

Tbmp Basalt of Mt. Pisgah (lower and upper Oligocene)—Brownish-gray- to medium-light-brown-weathering, dark-gray, massive pyroxene basalt. Contains aphanitic and agglutinous zones. The latter often contain zeolitic minerals. Thick, colluvial aprons are rare on Mt. Pisgah, generally only a thin veneer of soil covers these flows. Petrographically the basalt consists of a groundmass of seriate plagioclase to 1.5 mm with glass up to 50 percent and olivine and clinopyroxene phenocrysts from 1-4 mm. Olivine and pyroxene are commonly partially altered to iddingsite, chlorite or green smectite clay. Geochemically, the flows are basalt (Table 1, Map No.s M31, M32, M33, M34, M35, M36; Figure 3) and tholeiitic (Table 1, Figure 4). Although often containing large clinopyroxene phenocrysts, the basalt flows here are chemically different from petrographically similar flows at Camp Creek Ridge (Figure 3). The unit has no exposed contacts with other volcanic units and no isotopic ages, making stratigraphic relationships uncertain. Presumably, based upon a regional eastward younging of units, the basalt of Mt. Pisgah is somewhat younger than 30-Ma basalt at Springfield Quarry, and somewhat older than the 25.9 Ma tuff of Dexter.

Tpb Pyroxene basalt (lower and upper Oligocene)—Brown- to orange-weathering, dark-gray to dark-olive-gray, pyroxene basalt. Generally massive to tabular, also locally agglutinous. Distinguished by its large phenocrysts of pyroxene up to 1 cm, typically 4-5 mm. Petrographically consists of subhedral clinopyroxene 1-5 mm, rarely up to 1 cm, and plagioclase phenocrysts 1-2 mm in a groundmass of black glass and plagioclase microlites. Olivine can be a notable groundmass constituent, too, but is typically iddingsitized. Deeply weathered agglutinous zones are typically full of soft white opaque zeolites. Pyroxene phenocrysts often stand out as bumps on weathered surfaces. The unit upholds much of Camp Creek Ridge, with significant outcrops near Alder Branch in the Mohawk valley, Hayden Bridge, and Vitus Butte. Geochemically, the flows are basalt (Table 1, Map No.s M4, M6, M8, M12, M14, M16, M19; Figure 3) and tholeiitic (Table 1, Figure 4). Although both this unit and the basalt of Mt. Pisgah have large pyroxene phenocrysts, the two units populate different areas of the Ba-Sr diagram (Figure 7). The

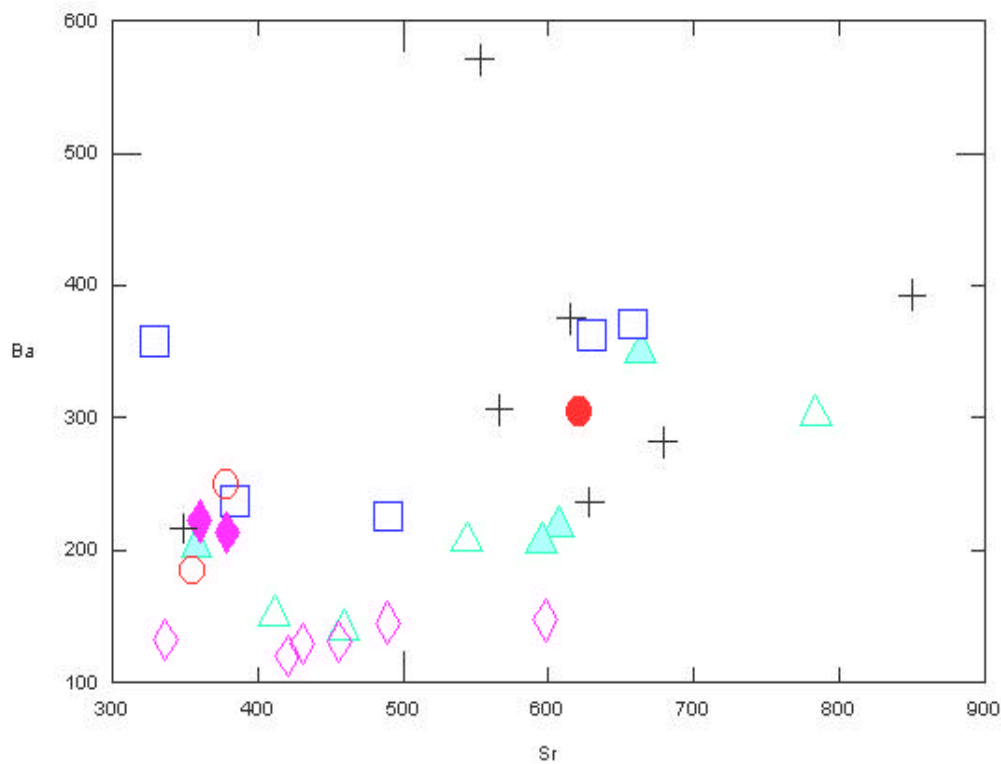


Figure 7. Plot of Ba vs. Sr for basaltic lava flows in the Springfield quadrangle. The plot accentuates chemical differences and similarities for flows that often have subtle petrographic differences. Notably the basalt of Mt. Pisgah and the pyroxene basalt are chemically distinct, even though both rock types often contain abundant large pyroxene phenocrysts. As shown above, Oligocene basalt and basalt of Camp Creek Ridge broadly overlap chemically—they are also similar petrographically. The basalt of Mohawk and the basalt of Camp Creek Ridge broadly overlap, and the basaltic andesites of Oligocene to Miocene age above the tuff of Dexter are quite close chemically in terms of Ba/Sr.

Legend:

Open green triangles:	Oligocene basalt	(unit Tb)
Closed green triangles:	Basalt of Camp Creek Ridge	(unit Tbac)
Open blue squares:	Basalt and andesite of Coburg Hills	(unit Tbah)
Closed blue squares:	Basalt of Mohawk	(unit Tbm)
Open purple diamonds:	Basalt of Mt. Pisgah	(unit Tbmp)
Closed purple diamonds:	Middle Miocene basaltic andesite	(unit Tmb)
Open red circles:	Oligocene-Miocene basaltic andesite	(unit Tomb)
Black crosses:	Pyroxene basalt	(unit Tpb)

unit is underlain by rhyolite and the basalt of Mohawk and is capped by the basalt of Camp Creek Ridge.

- Tv **Vent deposits (lower upper Oligocene)**—Reddish-brown, consolidated, often zeolitic agglutinous basaltic spatter and scoria. Petrographically the rock consists of sporadic fine-grained (<0.5 mm) plagioclase in a matrix of reddish-brown glass, clay, and iron-oxides. Geographically small (<7 acres) exposures are found on Camp Creek Ridge in secs. 2 and 23, T. 17 S., R. 2 W. where vegetation and soil cover are thin. The unit weathers readily producing subdued topography. In sec. 2, a narrow, northeast-trending , 0.3-m-wide dike less than 10 m long cuts the unit (Figure 8). Islands in a sea of pyroxene basalt, presumably these vent deposits are preserved source areas for the pyroxene basalt.
- Tvc **Volcaniclastic rocks (lower and upper Oligocene)**—Light-brown-weathering, varicolored reddish-brown, yellow, black, and tan, deeply weathered clayey volcanic sandstone, basaltic tuff, tuffaceous mud-supported basaltic conglomerate, and agglutinate on Camp Creek Ridge. Deposits typically are soft and penetratively weathered to saprolite consisting of weakly stratified clayey soil peds containing mixed scoria clasts, sporadic weathered angular basalt lithic boulders and subrounded pebbles and cobbles, and powders and coatings of manganese oxide and iron oxides on clasts and throughout the clayey, sandy matrix. Mapped in the northeast part of the quadrangle on Camp Creek Ridge, these deposits are prone to various types of slope failure including slumping, sliding, and creep. The unit is best exposed in the headwall scarps of slides and slumps and in deep roadcuts, but is generally heavily vegetated and poorly exposed. The unit is stratigraphically coeval with pyroxene basalt and capped by basalt of Camp Creek Ridge.



Figure 8. Erosion-resistant basaltic dike in agglutinous lava and scoria of unit Tv on Camp Creek Ridge.

Tbah **Basalt and andesite of Coburg Hills (lower and upper Oligocene)**—Commonly platy, glassy, orange- to tan-weathering, dark-olive-gray, fine-grained basalt and andesite lava flows capping the Coburg Hills. Where deeply weathered produces thick brown or reddish-brown saprolitic soils. Petrographically consists of seriate plagioclase to 1 mm, up to 20 percent dark glass, with olivine and clinopyroxene partially altered to iddingsite. Up to 5 percent celadonite in the groundmass. Geochemically, the flows range from basalt to andesite (Table 1, Map No.s M1, M2; Figure 3) and are tholeiitic (Table 1, Figure 4). The unit overlies rhyolite (unit Tr).



Figure 9. Palagonitized basalt of Mohawk (unit Tbm) exposed along Camp Creek Road. Below the hammer the rock is weathering spheroidally to a olive-gray and gold-colored grus-like fragments.

Tbm **Basalt of Mohawk (lower Oligocene)**—Grey to pale-olive-weathering, medium-gray to olive-gray, fine- to medium-grained tabular to blocky basalt. Contains local reddish-brown, zeolitic agglutinous zones. Petrographically consists of 10-20 percent olivine up to 3 mm with iddingsite rims, 5 percent clinopyroxene 1-2 mm, setting in a groundmass of 10-20 percent dark gray glass and seriate plagioclase less than 0.5 mm. Locally, in its lower part, weathers spheroidally to dark-olive-gray grus-like fragments with olivine and clinopyroxene altered to chlorite and/or green smectite clay and groundmass altered to pale olive to gold palagonite (Figure 9). Geochemically, the rock is basalt (Table 1, Map No.s M15, M17, M18; Figure 3) and tholeiitic (Table 1, Figure 4). Crops out at Vitus Butte-Hayden Bridge area at the base of Camp Creek Ridge. Overlies fossil-leaf-bearing clay-rich sandstone of the Fisher Formation near Hayden Bridge and is overlain by pyroxene basalt at Camp Creek Ridge.

Tr **Rhyolite (lower Oligocene)**—Light-gray to tan or orangish-brown-weathering, light-gray, light-pink, to pale-tan rhyolite (M7, M10, Table 1). Massive, resistant unit (where less altered) cropping out in the Coburg Hills (Figure 10) and the western lower flanks of Camp Creek Ridge at Stafford Creek. Typically chalky gray with abundant phenocrysts of plagioclase, lesser quartz and pyroxene, and traces of biotite in a fine-grained, usually argillized matrix. Often penetratively altered to light-colored clays. Locally silicified and



Figure 10. Orangish-brown-weathering, pale tan rhyolite in the Coburg Hills.

at one isolated locality in sec. 18, T. 17 S., R. 2 W., slightly mineralized with a trace of copper-iron sulfides. Dark reddish brown, vesicular, amygdaloidal and agglutinous at Sister Creek (Map No. M10). Geochemically, the flows are rhyolite to dacite in composition (Table 1, Map No.s M3, M7, M10; Figure 3) and predominantly tholeiitic (Table 1, Figure 4). Age unknown, bounded below by terrestrial volcaniclastic sediments that lie above the 31.3-Ma Spores Point Tuff (Madin and Murray, 2004) and Oligocene basalt (unit Tb) and above by the overlying basalt and andesite of Coburg Hills. In Camp Creek Ridge, overlain by pyroxene basalt. Thickness up to 305 m (1,000 ft).

Tb **Oligocene basalt and basaltic andesite with minor volcaniclastic sedimentary rocks (lower Oligocene)**—Dark-orangish-brown and light-gray-weathering, dark-gray and dark-greenish-gray, massive to tabular although locally reddish-brown and agglutinous olivine basalt and basaltic andesite. Lava flows locally interbedded with small discontinuous beds of sandy or pebbly claystone, clay-rich volcanic lithic sandstone, polymictic volcaniclastic subangular conglomerate or lahar deposits. Locally spheroidally

weathered and penetratively altered. Weathering of the unit produces thick colluvium with abundant subangular basalt fragments to boulder size in dark brown soil. Irregular zones of hard, partly palagonitized basalt cores of various sizes encased in massive to faintly stratified palagonitized, clayey ash and lithics are well exposed at Springfield Butte in sec. 1, T. 18 S., R. 3 W. in the adjacent Eugene East quadrangle. Petrographically the lava flows typically consist of a groundmass of fine-grained seriate plagioclase to 1.5 mm with glass and olivine and clinopyroxene phenocrysts from 1-2 mm. Olivine and pyroxene are commonly partially altered to iddingsite, chlorite or green smectite clay. Geochemically, the flows are basalt to basaltic andesite (Table 1, Map No.s M13, M22, M23, M24; Figure 3) and tholeiitic (Table 1, Figure 4). Mapped in the northwest part of the quadrangle at the base of the Coburg Hills and at Springfield Butte in sec. 1, T. 18 S., R. 3 W. The unit also upholds knolls in the Mt. Vernon area in the south central part of the quadrangle. Bounded at the base by volcanoclastic rocks that directly overlie the 31.6 Ma-tuff of Spores Point in the Coburg Hills and by the Fisher Formation at Springfield Butte (Madin and Murray, 2004). The unit in the Springfield quadrangle is equivalent to the lower part of unit Tb of Madin and Murray (2004), but not the upper part, which we call the basalt and andesite of Coburg Hills. The unit has a whole rock K/Ar date of 30.3 ± 1.1 Ma at the Springfield Butte quarry (Lux, 1981).

Tertiary (Eocene-Oligocene) Sedimentary Rocks

- Tf Fisher Formation (middle Eocene to upper Oligocene)**—Dark-tan-weathering, dark-gray to medium-tan, moderately-well to poorly sorted sandy mudstone; cobbly mudstone and conglomerate with subrounded to rounded, smoothed pebbles and cobbles; and muddy sandstone with angular crystals and volcanic lithics (2-4 mm). May often contain woody debris: leaves, bits and pieces of wood, logs. Typically massive with sporadic thin beds. Sporadic gravel is typically suspended in a muddy sandstone matrix. Abundant clay matrix and poorer sorting in sandstone beds distinguishes it from the marine Eugene Formation (Retallack, 2003, personal comm.). Consists of non-marine, fluvial facies in the Springfield quadrangle although significant components of volcanoclastic rocks are included in the Eugene area (Madin and Murray, 2004). Weathering of this unit generally produces thin colluvium and soil. Most exposures are found in the southeast part of the quadrangle along the Middle Fork of the Willamette River. There is, however, leaf-bearing volcanic lithic sandstone exposed in septic test pits in sec. 20, T. 17 S., R. 2 W. near Hayden Bridge. These exposures were also mapped by Maddox (1965), although there is little indication of the extent of these outcrops today because of grass-covered soils. The Fisher Formation is overlain by the basalt of Mohawk near Hayden Bridge, and by volcanoclastic rocks at Wallace Creek along the Willamette River. At Springfield Butte in sec. 1, T. 18 S., R. 3 W. the Fisher Formation is overlain by Oligocene basalt (unit Tb) at Springfield Quarry. Its bottom contact is not exposed in the map area. Madin and Murray (2004) indicate a time-transgressive unit spanning the interval from middle Eocene to Oligocene time; its occurrence above the tuff of Dexter indicates deposition as late as late Oligocene time. Peck and others (1964, p. 12) assigned similar rocks, in the Cascade Range near Eagle Point, Oregon, that lie above the rhyodacitic tuff of Bond Creek to the Little Butte Volcanics. The tuff of Bond Creek is a distinctive marker bed that has been tracked to the Eugene-Springfield area (Retallack and others, in Prep.)

Tertiary Intrusive Rocks

Tbd **Basaltic dikes (Oligocene and Miocene)**—Olive-brown-weathering, dark-gray to dark-olive-gray, very fine-grained, massive to tabular basalt dikes. Exposed at Wallace Creek in sec. 15 T. 18 S., R. 2 W. and in sec. 8, T. 17. S., R. 2 W., in the Coburg Hills. Petrographically consists of 7 percent iddingsitized olivine up to 0.5 mm with most less than 0.2 mm; 10-20 percent dark-greenish-gray glass, and 60-75 percent seriate plagioclase less than 0.5 mm. Geochemically, these dike rocks are basalt (Table 1, Map No. M38; Figure 3) and tholeiitic (Table 1, Figure 4). Near Wallace Creek, a dike cuts gently dipping sandstone of the Fisher Formation at a high angle. The contact, though mostly covered by soil, is abrupt. The contact with rhyolite in the Coburg Hills is similarly high angle but also associated with a fault.

STRUCTURE

The first order structure of the area is a gently northeast-dipping homocline. Strata dip measurably eastward with no radical variation, between 0 and 13 degrees. In general, rock ages are older in the west (30.3 ± 1.1 -Ma basalt, unit Tb) than in the east (18.0 ± 1.5 Ma-basaltic andesite, unit Tmba). This homoclinal structure is probably related to isostatic loading of the crust caused by volcanic accumulations of the Cascade Range immediately eastward.

Constructional volcanic accumulations modified by structural, primarily due to faults, and erosional complexities vary the geologic landscape. Prior investigators recognized the influence of faulting along the western front of the Coburg Hills (Lewis, 1951; Graven, 1990). Our mapping indicates that faulting has influenced the development of the Mohawk River valley. Volcanic units tend to be massive, lobate and lenticular in character, deposited on irregular surfaces and disconformably overlying sedimentary strata and other volcanic units, making strikes and dips difficult to measure. The Fisher Formation, however, provided dips where well-exposed massive and thick-bedded fluvial sandstones crop out along the Middle Fork of the Willamette River, although the massive bedding character, channeling, and the faintness of foreset beds made ascertaining actual bedding planes difficult.

Mapping faults in areas where beds are discontinuous and of irregular thickness where exposures are few requires supporting evidence and making inferences. No fault planes were found exposed. In the valley of the Mohawk River, rhyolite is in abrupt contact with basalt of Mohawk. The contact is linear and at a high-angle to the horizontal plane. It is inferred that the fault also lies beneath alluvium lining the Mohawk valley and played a role in the alignment of the valley. Short linear faults account for the abrupt, linear contacts at Vitus Butte and in the Hayden Bridge area. Faults in the highlands of Camp Creek Ridge in secs. 11 and 14, T. 17 S., R. 2 W. account for small offsets and abrupt terminations of the basalt of Camp Creek Ridge and the basalt of Mohawk. The basalt of Camp Creek Ridge is a ridge-capping unit that drapes pyroxene basalt that was deposited on the curvi-planar surface of an ancient volcano. Therefore we found the basalt of Camp Creek Ridge to cap the modern ridge but also to drape the east-sloping surfaces of ridge. This volcanic structure is now deeply eroded. Exposures of basalt of Camp Creek Ridge along the McKenzie River also reflect down-to-the south faulting. Faults in the Coburg Hills are derived from abrupt stratigraphic relationships and breccia zones in rhyolite. In secs. 5 and 8, T. 17 S., R. 2 W., a large basaltic dike is emplaced along a fault whose offset indicates valleyward offsets of rhyolite and downfaulting of basalt and andesite of Coburg Hills. Faults in these heavily forested upland areas probably continue farther than mapped.

Faults at Mt. Pisgah in the southwest corner of the map are derived from linear topographic and aerial photographic features integrated with, where exposed, abrupt changes from agglutinous to tabular lava beds.

Faults in the Wallace Creek area in the southeast corner of the map are derived from aerial photographic and field stratigraphic evidence. In secs. 14 and 15, T. 18 S., R. 2 W., beds of Fisher Formation, tuff of Dexter, and a basaltic dike are offset by a complex array of faults. In secs. 3 and 10, T. 18 S., R. 2 W., faults truncate the tuff of Dexter where it is overlain by canyon-filling basaltic andesite (unit Tmba). These faults also explain the often vertical juxtaposition of Fisher Formation and tuff of Dexter and indicate offsets in canyon-filling basaltic andesite (unit Tmba). Stratigraphic relationships indicate up to several hundred feet of throw where Miocene basaltic andesite is downdropped to the valley floor.

GEOLOGIC HISTORY

The geology of the Springfield quadrangle is concordant with a model that says from middle Eocene to late Oligocene time, an extensive fluvial-deltaic system eroding volcanic highlands of the Cascade volcanic arc to the east and south, debouched westward into the sea. The Fisher Formation provides evidence for this period of geologic history in the Springfield quadrangle, where the Fisher Formation is entirely non-marine and predominantly fluvial. To the west, however, it contains significant subaerial volcanoclastic lithologies, too, with volcanic sources mainly to the south (Madin and Murray, 2004). In the Springfield quadrangle we found that the Fisher Formation was deposited as late as late Oligocene time, because we find well-sorted fluvial facies above the 26-Ma tuff of Dexter (Figure 6).

The first-order eastward-dipping homoclinal structure of the region and the isotopic data provide the framework for understanding its Tertiary geologic history. Isotopic ages of pyroclastic rocks near the west edge of the Springfield quadrangle indicate their emplacement between 32 and 30 Ma. These include the 32-Ma tuff of Daniels Creek in the Coburg Hills (Figure 2, Table 2, map no. 5,) and 32-Ma Mosser Mountain tuff of Retallack and others (in Prep.) at Short Mountain (Figure 2, Table 2, map no. 4), the 31-Ma tuff of Spores Point at the McKenzie River and Goshen (Figure 2, Table 2, map no.'s 2, 3) and the 31-Ma tuff of Willamette Flora at Goshen (Figure 2, Table 2, map no. 17). Rocks east of the map area are younger than those to the west. Basaltic rocks near Camp Creek (Figure 2, Table 2, map no. 11) and Marcola (Figure 2, Table 2, map no.'s 10, 13, 15) were emplaced 29 to 27 Ma. Dated rocks that crop out within the map area include 30-Ma basalt at Springfield quarry at the west edge of the map (Figure 2, Table 2, map no. 16), the 26-Ma tuff of Dexter (Figure 2, Table 2, map no. 1), and 18-Ma basaltic andesite from the Natron quarry (Figure 2, Table 2, map no. M28). Thus the known ages for rocks within the map area also reflect an eastward younging.

The oldest rocks in the quadrangle are Fisher Formation sedimentary rocks at Springfield Butte overlain by 30-Ma basalt (unit Tb). The Fisher Formation at Springfield Butte is not well exposed within the quadrangle itself, but exemplary exposures are located less than 100 m to the west in the Eugene East Quadrangle. Pebbles, cobbles, and immature clayey volcanic lithic sandstones in the Fisher Formation all indicate a volcanic provenance. Contacts with overlying basaltic units are not well exposed, but map relations do not indicate major angular unconformities. Instead, it appears that basaltic lavas were intermittently deposited on fluvial Fisher Formation sands during Oligocene time. Pillow basalts were not found in the map area, however, locally overlying basaltic units, such as the basalt of Mohawk, are spheroidally weathered and palagonitically altered to crumbly grus-like fragments (Figure 9) indicating

possible initial water-lava interaction. Much alteration of the rocks is masked, however, by the deep, penetrative saprolitic weathering that affects so many of the rocks in the area.

At the south end of the Coburg Hills, at what is now the valley of the Mohawk River, viscous rhyolitic flows (unit Tr) erupted onto Oligocene basalt flows (unit Tb). Locally, the rhyolite is vesicular and amygdaloidal, indicating subaerial emplacement. Rhyolite is not a far-traveled extrusive rock—sources must have been local, probably within the map area. Intense argillic alteration, penetrative weathering, and thick vegetation, however, have covered evidence of source features such as dikes or ring fractures. Argillic alteration, local silicification and the minute amount of copper sulfide discovered, indicate local and limited hydrothermal alteration.

Overlying the rhyolite are flows of pyroxene basalt (unit Tpb) and basalt and andesite of Coburg Hills (Tbah). Vent rocks (Tv) and volcanoclastic rocks (Tvc) are associated with the pyroxene basalt lavas at Camp Creek Ridge. Pyroxene basalt was capped by fine-grained basalt of Camp Creek Ridge (unit Tbac). Camp Creek Ridge is the eroded remains of what became a major basaltic edifice during late Oligocene time. Presumably, although there is no direct evidence for this, basalt lava was emplaced at Mt. Pisgah at about the same time.

In the late Oligocene, 26-Ma, the tuff of Dexter was deposited. Large, Plinian-style eruptions from sources to the southeast (Retallack, 2003, personal comm.) generated pumice-rich ignimbrite clouds that carpeted the landscape and filled ancient valleys to depths of up to 200 m (600 ft) (Retallack, 2003, personal comm.). The tuff of Dexter was the last of a series of major ignimbrites deposited in the region between middle Eocene and late Oligocene time (Retallack and others, in Prep.). These tuff beds have become useful stratigraphic markers for mapping (Retallack and others, in Prep.; Madin and Murray, 2004). The tuff of Dexter is the only major tuff exposed in the Springfield quadrangle—other major ignimbrites are exposed to the west and south (Retallack and others, in Prep.; Madin and Murray, 2004).

The tuff of Dexter was deposited on fluvial pebbly sandstones of the Fisher Formation. The ignimbrite was evidently following the paleovalley of an ancient river. Once the tuff cooled, the river re-established itself upon the tuff. The top of the tuff was scoured and conglomerate beds with rounded cobbles and pebbles and sandstone were deposited atop the tuff of Dexter (Figure 6). Hence, the tuff of Dexter is sandwiched within the Fisher Formation, much as are ignimbrites lower in the stratigraphic section to the west and south (Retallack and others, in Prep.; Madin and Murray, 2004).

In latest Oligocene time, the upper part of the Fisher Formation was subsequently locally incised and overlain by channel-fill and sheetwash volcanoclastic deposits at Wallace Creek (unit Twc). Basaltic highlands to the east, perhaps only a few kilometers away, provided the source material. Lithologies indicate a mixture of lahar, debris flow, fluvial (small-stream), and hillside outwash deposits. The terrain must have been wooded—petrified wood is locally abundant.

The volcanoclastic rocks at Wallace Creek were subsequently inundated by basaltic andesite lava flows (unit Tomb) during latest Oligocene time. The sources were probably nearby and to the east. These now deeply weathered flows were incised to several hundred feet. During middle Miocene time basaltic andesite filled canyons (unit Tmba). Locally, the lava cooled to well-formed columns. Post-18-Ma faulting offset these Miocene flows.

The region underwent continued gradual uplift and erosion. Tertiary valley fill is now preserved as remnant terrace gravel (unit QTg) above the modern valley floor. The deposits are penetratively weathered with rounded cobbles and pebbles decomposed to soft “porphyritic” clay clasts. These gravels represent Willamette valley fluvial deposits of probable Pliocene and younger age. These gravels were subsequently incised to depths of many tens of feet. After a period of incision, the Willamette Valley and tributary valleys, such as that of the Mohawk River, underwent refilling during Pleistocene time. Braided-fan gravels spread out and accumulated across the Willamette Valley floor.

Today, the modern streams and rivers are incising older gravel and bedrock deposits and redistributing and redepositing alluvial deposits. The Mohawk River is now well-entrenched in its

bed, commonly cutting 3-6 m (10-20 ft) into older gravels. On the alluvial plains, the McKenzie and Willamette Rivers have banks up to 5 m (15 ft) high. In the east side of the map area, however, the McKenzie River is aggrading its bed—its banks are low, the channels anastomosing, and the beds are full of gravel. All of the rivers have come out of their banks in historical times, flooding broad areas of their valleys as recently as 1964.

Many of the bedrock units of the Springfield quadrangle are deeply weathered to saprolitic soils, particularly in the Coburg Hills, Camp Creek Ridge, and east of Jasper. The decomposition of these bedrock units has led to the development of numerous landslides, deep colluvium, and alluvial fans. These, in turn, are being eroded and supply sediment for the long-lived McKenzie-Willamette fluvial system.

ACKNOWLEDGEMENTS

The authors express their appreciation for Dr. Greg Retallack of the University of Oregon for numerous insightful discussions, for Steve and Ben Newcomb of EGR Associates for float-trip assistance with geology on the McKenzie River, to Jeanne Hunt of Weyerhaeuser and Bob Sward of Giustina Land & Timber Co. for keys to their company's private timberlands, for numerous unnamed landowners who patiently permitted access, for Bob Murray of the Oregon Department of Geology and Mineral Industries for field trips, and for Bob and Joan Hladky whose property near Springfield provided a welcome field station for the authors after long days in the field.

REFERENCES

- Abbey, S., 1983, Studies in "standard samples" of silicate rocks minerals 1969-1982: Geological Survey of Canada Paper 83-15, p.1-114.
- Berggren, W.A., Ken, D.V., Flynn, J.J., and Van Couvering, J.A., 1985, Cenozoic geochronology: Geological Society of America Bulletin, v. 96, no. 11, p. 1,407-1,418.
- Cebula, G.T., Kunk, M.J., Mehnert, H.H., Naeser, C.W., Obradovich, J.D., and Sutter, J.F., 1986, The Fish Canyon Tuff, a potential standard for the ^{40}Ar - ^{39}Ar and fission-track dating methods (abstract), Terra Cognita (6th Int. Conf. on Geochronology, Cosmochronology and Isotope Geology), v. 6, p. 139-140.
- Evernden, J.F., and James, G.T., 1964, Potassium-argon dates of the Tertiary floras of North America: American Journal of Science, v. 262, p. 945-974.
- Fiebelkorn, R.B., Walker, G.W., MacLeod, N.S., McKee, E. H., and Smith, J.G., 1983, Index to K-Ar age determination for the State of Oregon: Isochron West, no. 37, p. 3-60.
- Govindaraju, K., 1994, Compilation of working values and sample description for 383 geostandards: Geostandards Newsletter, v. 18, Special Issue, p. 1-158.
- Graven, E.P., 1990, Structure and tectonics of the southern Willamette Valley, Oregon: Unpublished MSc thesis, Oregon State University, Corvallis, 119 p.
- Hickman, C.J.S., 1969, The Oligocene marine molluscan fauna of the Eugene Formation in Oregon: Museum of Natural History, University of Oregon, Bulletin 16.
- Hladky, F.R., 1992, Geology and mineral resources map of the Shady Cove quadrangle, Jackson County, Oregon: Oregon Department of Geology and Mineral Industries Geological Map Series GMS-52, scale 1:24,000

- Irvine, T.N., and Baragar, W.R.A., 1971, A guide to the chemical classification of the common volcanic rocks: *Canadian Journal of Earth Sciences*, v. 8, no. 5 p. 523-548.
- Le Bas, M.J., and Streckeisen, A.L., 1991, The IUGS systematics of igneous rocks: London, *Journal of the Geological Society*, v. 148, p. 825-833.
- Lewis, R.Q., 1951, The geology of the southern Coburg Hills, including the Springfield- Goshen area: Unpublished MSc thesis, University of Oregon, Eugene, 58 p., scale 1:62,500.
- Lux, D.R., 1981, K-Ar and $^{40}\text{Ar}/^{39}\text{Ar}$ ages of mid Tertiary volcanic rocks from the western Cascade Range, Oregon: *Isochron West*, v. 33, p. 27-32.
- Madin, I.P., and Hladky, F.R., in Prep., Preliminary geologic map of the Coburg Quadrangle, Lane County, Oregon.
- Madin, I.P., and Murray, R.B., 2004, Preliminary geologic map of the Eugene East and Eugene West Quadrangles, Lane County, Oregon: *in* Oregon Department of Geology and Mineral Industries Open-File Report O-03-11.
- Maddox, T., 1965, Geology of the southern third of the Marcola Quadrangle, Oregon: Unpublished MSc thesis, University of Oregon, Eugene, 78 p.
- Millhollen, G.L., 1991, Welded tuffs of the Winberry Creek area, central Oregon Cascade Range: *Oregon Geology*, v. 53, p. 89-91.
- Murray, R.B., 1994, Geology and mineral resources of the Richter Mountain 7.5-minute Quadrangle, Douglas and Jackson Counties, Oregon: Unpublished MSc thesis, University of Oregon, Eugene, 239 p.
- O'Connor, J.E., Sarna-Wojcicki, A., Wozniak, K.C., Polette, D.J., and Fleck, R.J., 2001, Origin, extent, and thickness of Quaternary geologic units in the Willamette Valley, Oregon: U.S. Geological Survey Professional Paper 1620, 52 p., scale 1:250,000.
- Peck, D.L., 1960, Geologic map of the western Cascades: U.S. Geological Survey Open-File Report OFR-60-110, scale 1:200,000.
- Peck, D.L., Griggs, A.L., Schlicker, H.G., Wells, F.G., and Dole, H.M., 1964, Geology of the central and northern parts of the Western Cascade Range in Oregon: U.S. Geological Survey Professional Paper 449, 56 p.
- Reichen, L.E., and Fahey, J.J., 1962, An improved method for the determination of FeO in rocks and minerals including garnet: U.S. Geological Survey Bulletin 1144B, p. 1-5.
- Retallack, G.J., Prothero, D.P., Duncan, R.A., and Ambers, C.P., in Prep., Eocene-Oligocene extinctions and paleoclimatic change near Eugene, Oregon.
- Staudacher, T.H., Jessberger, E.K., Dorflinger, D., and Kiko, J., 1978, A refined ultrahigh-vacuum furnace for rare gas analysis, *Journal of Physics E: Scientific Instruments*, v. 11, p. 781-784.
- Steven, T.A., H.H. Mehnert, and J.D. Obradovich, 1967, Age of volcanic activity in the San Juan Mountains, Colorado, U.S. Geological Survey Professional Paper, 575-D, p. 47-55.
- Vokes, H.E., Snively, P.D., and Myers, D.A., 1951, Geology of the southern and western border areas, Willamette Valley, Oregon: USGS Oil and Gas Investigation Map, OM-110, 1 p.
- Walker, G.W., and Duncan, R.A., 1989, Geologic map of the Salem 1° x 2° sheet, Western Oregon: USGS Miscellaneous Investigations Map I-1893, scale 1:250,000.

- Wendt, I., and Carl, C., 1991, The statistical distribution of the mean squared weighted deviation, *Chemical Geology*, v. 86, p. 275-285.
- Yeats, R.S., Graven, E.P., Werner, K.S., Goldfinger, C., and Popowski, T., 1996, Tectonics of the Willamette Valley, Oregon, in Rogers, A.M., and others., eds., *Assessing earthquake hazards and reducing risk in the Pacific Northwest: U.S. Geological Survey Professional Paper 1560*, p. 183-222.

APPENDIX A—

Additional Sample Descriptions/Locations, Springfield Quadrangle

Selected samples were analyzed (see Table 1).

General Location	Lithology	Sample No.	UTM_N	UTM_E
69th Street	altered basaltic andesite?	SF137	4875425	509467
	granule conglomerate	SF136	4876087	509545
Camp Creek Ridge	agglutinate	SF25	4884243	508300
	altered basaltic andesite	SF96	4883064	508691
	altered porphyritic basalt	SF20A	4885112	508935
	basalt	SF6	4879417	504292
	basaltic agglutinate	SF20B	4885417	508856
		SF22	4885518	508683
		SF27	4883480	508660
		SF9	4883261	508964
	basaltic andesite	SF100	4883497	509479
		SF23	4884000	508840
		SF26	4883890	508980
		SF28	4883606	509180
		SF97	4883328	508632
		SF98	4882962	508645
		SF99	4882722	509078
	basaltic float	SF17	4884041	507561
	coarse weathered clastics	SF107	4880947	507506
Camp Creek Ridge	highly altered basalt	SF24	4884000	508840
	pyroxene basalt	SF10	4882568	508531
		SF101	4883893	509740
		SF102	4883917	509694
		SF103	4881272	508056
		SF104	4881050	508007
		SF105	4880864	507966
		SF106	4880339	507682
		SF12	4884746	508101
		SF13	4884796	507929
		SF14	4884597	507476
		SF15	4884540	507460
		SF16	4884398	507502
		SF21	4885477	508707
	pyroxene basalt agglutinate	SF11	4883904	508126
	sandy claystone	SF18	4884528	508867
	tuffaceous conglomerate	SF19	4884884	508971
Coast Fork Willamette River	pyroxene basalt	SF69	4870583	503196
Coburg Hills	agglutinate	SF64	4884421	499971
	altered agglutinate	SF63	4884540	500120
	altered basalt?	SF66	4885045	500515
		SF67	4884379	501380
Coburg Hills	altered basaltic andesite	SF68	4884480	503044
	altered basaltic andesite?	SF49	4884855	502075
	basalt	SF108	4884106	504660
		SF110	4884351	504050
		SF2	4881050	500092
		SF3	4884560	500060
		SF33	4883631	500992
		SF34	4883629	500927
		SF35	4883116	500693
		SF37	4883084	500587
		SF38	4883111	500276
		SF39	4882517	500225
		SF43	4881100	500340
		SF44	4881074	500318
		SF60	4884050	501887
		SF94	4884308	499627
		SF95	4883073	498433
	basaltic agglutinate	SF53	4885189	502374
		SF54	4885124	502373
		SF62	4884600	500100
	basaltic andesite	SF51	4884442	502559

General Location	Lithology	Sample No.	UTM_N	UTM_E
Coburg Hills	basaltic andesite	SF55	4885010	502388
		SF65	4884189	500080
	celadonic basalt dacite	SF70	4883930	501519
		SF109	4883150	504330
		SF111	4883460	504631
		SF61	4883930	501519
	fine grained basalt	SF93	4884207	501910
		SF89	4885262	501216
		SF90	4885355	501975
		SF91	4885550	501551
		SF92	4884206	501898
		SF92A	4884207	501906
	fine grained basaltic andesite	SF50	4884808	502139
		SF52	4885403	502206
		SF88	4884863	501990
	rhyodacite	SF36	4883033	500677
		SF4	4883333	501380
		SF42	4881503	500057
		SF45	4881580	502147
		SF46	4881881	502740
		SF47	4882343	503003
		SF48	4882406	503357
		SF5	4882679	502691
	silicified dacite	SF40	4882470	500171
	silicified dacite (float)	SF41	4882470	500131
Mc Kenzie River	altered basaltic agglutinate basalt	SF31	4879684	505034
		SF29	4878726	509269
	basaltic andesite	SF30	4879475	507690
		SF32	4879331	504293
Middle Fork Willamette River	basalt	SF56	4874238	502848
	pyroxene basalt	SF57	4874405	501593
Mt. Pisgah	altered basalt	SF160	4872138	503207
	altered basaltic agglutinate	SF85	4872815	502670
	amygdaloidal basalt	SF152	4871882	501975
	basalt (dike)	SF77	4873176	502190
	basaltic agglutinate	SF73	4873344	501552
		SF74	4873210	501864
		SF76	4873473	502277
		SF78	4872919	502414
		SF78A	4873111	502421
		SF79	4873050	502500
		SF80	4872900	502597
		SF81	4872627	502885
		SF84	4872524	502688
	basaltic andesite	SF151	4871726	502016
		SF155	4872609	502175
		SF71	4872519	501604
		SF72	4873252	501647
		SF82	4872302	502971
		SF83	4872399	502772
		SF149	4871435	502257
		SF75	4873464	502093
		SF162	4871841	503735
		SF156	4872579	502258
		SF157	4872700	502210
		SF158	4872733	501561
		SF159	4872108	503373
		SF161	4872243	503150
		SF74A	4873240	501622
		SF86	4872581	502548
		SF87	4873382	501491
	pyroxene basalt agglutinate	SF150	4871437	502237
		SF153	4871981	502038
		SF154	4872454	502134
Mt. Vernon	basaltic andesite	SF135	4875538	504128
		SF139	4876039	503285
Short Mountain	silicified dacite	SF1	4867703	500090

General Location	Lithology	Sample No.	UTM_N	UTM_E
Wallace Creek	basalt	SF142	4874427	508574
	basaltic andesite	SF143	4874380	508633
		SF145	4874519	508647
		SF146	4874978	508892
		SF147	4875032	508408
	brown tuff	SF138	4875112	508263
		SF140	4874808	508311
		SF148	4875070	508251
	fine grained basalt	SF141	4874417	508545
	granule conglomerate	SF144	4874314	508579
	basalt (dike)	SF112	4871894	507914
	basaltic andesite	SF8	4874930	507596
	Dexter tuff	SF118	4872524	506926
		SF119	4872524	506926
		SF7	4874545	507819
	Wallace Crk. volcanics	SF113	4873200	508407
		SF114	4874682	507992
		SF115	4874627	507977
		SF116	4874528	507864
		SF117	4874494	507738
		SF117A	4874167	507444
		SF120	4874400	507520
		SF121	4873031	506575
		SF122	4873290	507055
		SF123	4873080	507134
		SF124	4872788	507442
		SF125	4872763	507445
		SF126	4872667	507295
		SF127	4872730	507416
		SF128	4872478	507736
		SF129	4872539	507464
		SF130	4874650	508120
		SF131	4874559	508139
		SF132	4874559	508149
		SF133	4874483	508187
		SF134	4874271	508391

APPENDIX B—

Major and Minor Element Analyses

Sample preparation

Coarse rock fragments were crushed in a Bico Corporation alumina-plate equipped mullite grinder and a Spex shatter box equipped with a ceramic grinding vessel. All rock powder was ground to <80 mesh. Lithium tetraborate in the amount of 3.6000 ± 0.0002 grams was placed in a clean glass bottle with 0.4000 ± 0.0001 grams of the rock powder and mixed for 10 minutes in a Spex Mixer Mill. The homogenous powder was transferred into a lidded, 25-cc platinum (95%)-gold (5%) crucible with three drops of 2% Lil solution (to reduce viscosity) and heated, with the lid on, over a Meeker burner. The molten sample was poured and cast into the crucible lid, forming a 29-mm diameter disk.

It normally took 10 minutes to melt the rock powder. The powder was vigorously stirred during heating. Near the end of heating, the lid of the crucible was removed and heated over a Meeker burner unit it was red-hot. Then the crucible's contents were poured onto the hot lid.

Immediately upon completing pouring, the still hot crucible was placed into a beaker containing enough 4N HCl to cover the crucible.

On the other hand, the lid was placed flat on a surface to cool. The molten rock would freeze to a glass. In 3 to 5 minutes glass disk was cool enough to label the curved side with a magic marker. The resulting disk can be stored indefinitely in a desiccator. The disk was analyzed for the major elements and Sr, Zr, Cr, and V.

A slightly different procedure was done for preparing sample for trace element analysis. Whole rock powder in the amount of 7.0000 ± 0.0001 grams was mixed for 10 minutes with 1.4000 ± 0.0002 grams of high purity microcrystalline cellulose. The mixture was then pressed into a briquette. If the SiO₂ content of the whole rock was greater than 55%, copolywax powder was substituted for the cellulose. The elements measured from the briquette included Rb, Sr, Y, Zr, Nb, Ni, Ga, Cu, Zn, U, Th, Co, Pb, Sc, Cr, and V. La, Ce, and Ba were determined by using an L X-ray line and a mass absorption correction.

XRF Methodology

Whole-rock analyses for major and trace elements were performed using a Phillips 2404 X-ray fluorescence vacuum spectrometer equipped with a 102-position sample changer. Working curves for each element of interest were determined by analyzing 55 geochemical rock standards. Accepted chemical data for each of these rock standards has been synthesized by Abbey (1983) and Govindaraju (1994). Between 30 and 55 data points were gathered for each working curve, and various elemental interferences were taken into account. The Rh Compton peak was utilized for a mass absorption correction. Slope and intercept values, together with correction factors for the various wavelength interferences, were calculated and stored on computer.

Loss on Ignition (LOI) was determined by heating pre-weighed rock powder to 950° C for one hour, and then re-weighing the sample to determine the relative percentage of weight loss.

The amount of ferrous Fe was titrated using a modified Reichen and Fahey (1962) method.

APPENDIX C—

Isotopic Age Analysis

Sample Procedure

Samples analyzed by the $^{40}\text{Ar}/^{39}\text{Ar}$ method at the Nevada Isotope Geochronology Laboratory at University of Nevada, Las Vegas were wrapped in Al foil and stacked in 6 mm inside diameter Pyrex tubes. Individual packets averaged 3 mm thick and neutron fluence monitors (FC-2, Fish Canyon Tuff sanidine) were placed every 5-10 mm along the tube. Synthetic K-glass and optical grade CaF_2 were included in the irradiation packages to monitor neutron induced argon interferences from K and Ca. Loaded tubes were packed in an Al container for irradiation. Samples were irradiated at McMaster Nuclear Reactor at McMaster University, Ontario, Canada. The samples were in-core for 7 hours in the 5C position where they are surrounded by fuel rods on all four sides. Correction factors for interfering neutron reactions on K and Ca were determined by repeated analysis of K-glass and CaF_2 fragments. Measured $(^{40}\text{Ar}/^{39}\text{Ar})_{\text{K}}$ values were $0.0001 (\pm 100\%)$. Ca correction factors were $(^{36}\text{Ar}/^{37}\text{Ar})_{\text{Ca}} = 2.67 (\pm 3.83) \times 10^{-4}$ and $(^{39}\text{Ar}/^{37}\text{Ar})_{\text{Ca}} = 7.00 (\pm 0.63\%) \times 10^{-4}$. J factors were determined by fusion of 3-5 individual crystals of neutron fluence monitors which gave reproducibility's of 0.05% to 0.35% at each standard position. Variation in neutron flux along the 100 mm length of the irradiation tubes was $<0.2\%$.

Irradiated crystals together with CaF_2 and K-glass fragments were placed in a Cu sample tray in an high vacuum extraction line and were fused using a 20 W CO_2 laser. Sample viewing during laser fusion was by a video camera system and positioning was via a motorized sample stage. Samples analyzed by the furnace step heating method utilized a double vacuum resistance furnace similar to the Staudacher and others (1978) design. Reactive gases were removed by a single MAP and two GP-50 SAES getters prior to being admitted to a MAP 215-50 mass spectrometer by expansion. The relative volumes of the extraction line and mass spectrometer allow 80% of the gas to be admitted to the mass spectrometer for laser fusion analyses and 76% for furnace heating analyses. Peak intensities were measured using a Balzers electron multiplier by peak hopping through 7 cycles; initial peak heights were determined by linear regression to the time of gas admission. Mass spectrometer discrimination and sensitivity was monitored by repeated analysis of atmospheric argon aliquots from an on-line pipette system. Measured $^{40}\text{Ar}/^{36}\text{Ar}$ ratios were $290.74 \pm 0.22\%$ during this work, thus a discrimination correction of 1.01636 (4 AMU) was applied to measured isotope ratios. The sensitivity of the mass spectrometer was $\sim 6 \times 10^{-17} \text{ mol mV}^{-1}$ with the multiplier operated at a gain of 52 over the Faraday. Line blanks averaged 2.33 mV for mass 40 and 0.01 mV for mass 36 for laser fusion analyses and 2.54 mV for mass 40 and 0.006 mV for mass 36 for furnace heating analyses. Discrimination, sensitivity, and blanks were relatively constant over the period of data collection. Computer automated operation of the sample stage, laser, extraction line and mass spectrometer as well as final data reduction and age calculations were done using LabSPEC software written by B. Idleman (Lehigh University). An age of 27.9 Ma (Steven and others., 1967; Cebula and others., 1986) was used for the Fish Canyon Tuff sanidine flux monitor in calculating ages for samples.

For $^{40}\text{Ar}/^{39}\text{Ar}$ analyses a plateau segment consists of 3 or more contiguous gas fractions having analytically indistinguishable ages (i.e. all plateau steps overlap in age at $\pm 2\sigma$ analytical error) and comprising a significant portion of the total gas released (typically $>50\%$). Total gas (integrated) ages are calculated by weighting by the amount of ^{39}Ar released, whereas plateau ages are weighted by the inverse of the variance. For each sample inverse isochron diagrams are

examined to check for the effects of excess argon. Reliable isochrons are based on the MSWD criteria of Wendt and Carl (1991) and, as for plateaus, must comprise contiguous steps and a significant fraction of the total gas released. All analytical data are reported at the confidence level of 1σ (standard deviation).

Sample Description

SF-8 Basalt groundmass

This sample produced a discordant age spectrum, with rising ages from ~2 Ma to ~28 Ma. There was no plateau age obtained; the total gas age (equivalent to a K/Ar age) is 17.6 ± 0.5 Ma. A statistically valid isochron was obtained for steps 2-5 (~53% of the total gas released), indicating an age of 18.0 ± 1.5 Ma, and initial argon indistinguishable from atmospheric argon. The isochron age is quite imprecise due to the very low radiogenic yields (% $^{40}\text{Ar}^*$), causing all data to cluster near the y-axis. In addition, the spread in radiogenic yield is very low, thus all data cluster in one small area on the isochron, further reducing its usefulness for age constraints. The isochron does add some confidence to the total gas age (i.e. no excess argon is present in the sample). The low radiogenic yields, and discordant age spectrum, however, suggest the sample may be somewhat altered. The most conservative interpretation of these data is that the maximum measured age of ~28 Ma is the oldest possible age for the sample, as even the maximum age may reflect partial argon loss.

SF-8, basalt groundmass, 20.66 mg, J = $0.001669 \pm 0.40\%$

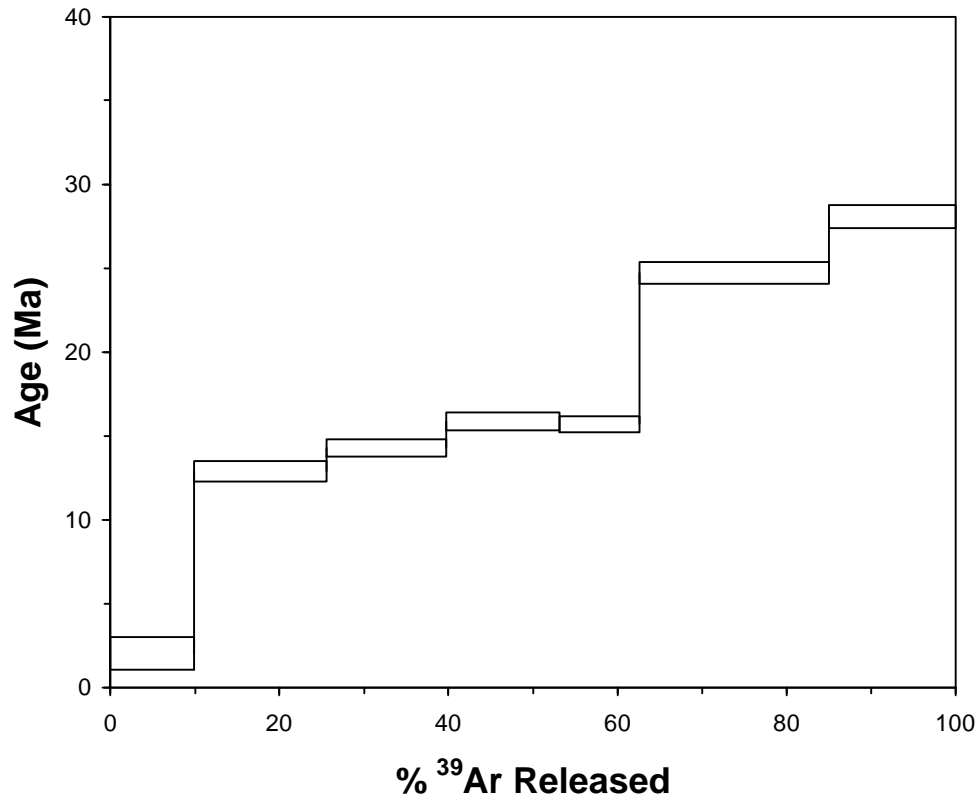
4 amu discrimination = $1.01636 \pm 0.22\%$, 40/39K = $0.0001 \pm 100.0\%$, 36/37Ca = $0.000267 \pm 3.83\%$, 39/37Ca = $0.00070 \pm 0.63\%$

step	T (C)	t (min.)	36Ar	37Ar	38Ar	39Ar	40Ar	%40 Ar	% 39Ar rlsd	Ca/K	40Ar*/39Ar K	Age (Ma)	1s.d.
1	830	12	8.547	13.890	2.486	9.856	2491.220	0.3	9.9	8.3705785	0.6742	2.03	0.99
2	890	12	8.496	31.288	2.800	15.490	2531.700	2.6	15.6	12.010314	4.2950	12.89	0.62
3	950	12	5.430	37.215	2.007	14.032	1638.130	4.0	14.1	15.787664	4.7651	14.29	0.52
4	1010	12	3.986	38.223	1.749	13.358	1215.980	5.7	13.5	17.039842	5.2892	15.86	0.55
5	1075	12	2.695	29.052	1.278	9.342	825.877	5.8	9.4	18.527281	5.2400	15.71	0.47
6	1150	12	7.253	163.593	3.348	22.278	2256.930	8.0	22.4	44.083056	8.2657	24.72	0.64
7	1400	12	2.545	250.399	1.363	14.883	825.406	16.3	15.0	102.76041	9.3957	28.07	0.69
Cumulative %39Ar rlsd =									100.0	Total gas age = 17.61 0.45			

note: isotope beams in mV, rlsd = released, error in age includes 0.5% J error, all errors 1 sigma
(36Ar through 40Ar are measured beam intensities, corrected for decay for the age calculations)

no plateau
no isochron

SF-8 - basalt groundmass



SF-8 - basalt groundmass

